

Noname manuscript No.  
(will be inserted by the editor)

# Quasi-Arithmetic Mixtures, Divergence Minimization, and Bregman Information

Rob Brekelmans · Frank Nielsen

Received: date / Accepted: date

**Abstract** Markov Chain Monte Carlo methods for sampling from complex distributions and estimating normalization constants often simulate samples from a sequence of intermediate distributions along an *annealing path*, which bridges between a tractable initial distribution and a target density of interest. Prior works have constructed annealing paths using quasi-arithmetic means, and interpreted the resulting intermediate densities as minimizing an expected divergence to the endpoints. To analyze these variational representations of annealing paths, we extend the results of Banerjee et al. [11] showing that the arithmetic mean over arguments minimizes the expected Bregman divergence to a single representative point. In particular, we obtain an analogous result for quasi-arithmetic means, when the inputs to the Bregman divergence are transformed under a monotonic embedding function. Our analysis highlights the interplay between quasi-arithmetic means, parametric families, and divergence functionals using the rho-tau Bregman divergence framework of Zhang [86, 87], and associates common divergence functionals with intermediate densities along an annealing path.

**Keywords** Bregman divergence · monotone embedding · quasi-arithmetic means / mixtures · non-parametric information geometry · gauge freedom · annealing paths · Markov Chain Monte Carlo

---

Rob Brekelmans  
Vector Institute  
University of Southern California Information Sciences Institute  
E-mail: rob.brekelmans@vectorinstitute.ai

Frank Nielsen  
Sony Computer Science Laboratories Inc,  
E-mail: frank.nielsen@acm.org

## 1 Introduction

Markov Chain Monte Carlo (MCMC) methods such as annealed importance sampling (AIS) [60], Sequential Monte Carlo (SMC) [28], thermodynamic integration (TI) [70, 38] and Parallel Tempering (PT) [30] are fundamental tools in statistical physics and machine learning, which can be used to sample from complex distributions, estimate normalization constants, and calculate physical quantities such as entropy or free energy. Such tasks appear in the context of Bayesian inference or model selection, where the posterior over latent variables or model parameters is usually intractable to sample and evaluate.

MCMC algorithms often decompose these problems into a sequence of easier subproblems along an *annealing path* of intermediate densities  $\{\tilde{\pi}_{\beta_t}(x)\}_{t=0}^T$ , which bridge between a tractable (often normalized) density  $\tilde{\pi}_0(x)$  and the complex target density of interest  $\tilde{\pi}_1(x)$ . Using the notation  $\tilde{\pi}$  to indicate the density of an unnormalized measure with respect to the Lebesgue measure, we are interested in sampling from  $\pi_1(x) \propto \tilde{\pi}(x)$  or estimating the normalization constant  $\mathcal{Z}_1 = \int \tilde{\pi}_1(x)dx$ , its logarithm  $\log \mathcal{Z}_1$ , or the ratio  $\mathcal{Z}_1/\mathcal{Z}_0$ , where  $\mathcal{Z}_0 = \int \tilde{\pi}_0(x)d(x)$ . Transition kernels  $\mathcal{T}_t(x_t|x_{t-1})$  such as importance resampling, Langevin dynamics [74, 83], Hamiltonian Monte Carlo (HMC) [29, 61, 14], and accept-reject steps are used to transform samples to more accurately simulate the target density. For example, we describe the annealed importance sampling algorithm (AIS, [60, 44]) in [Alg. 1](#), which provides approximate target samples and an unbiased estimator of the ratio of normalization constants.

Most commonly, intermediate unnormalized densities are constructed using geometric averaging  $\tilde{\pi}_\beta^{(\text{geo})}(x) = \tilde{\pi}_0(x)^{1-\beta} \tilde{\pi}_1(x)^\beta$  of the initial and target densities, with  $\beta \in [0, 1]$ . Viewing the geometric path as a quasi-arithmetic mean [49] under transformation by the natural logarithm, Masrani et al. [54] propose annealing paths using the deformed logarithm transformation function rooted in nonextensive thermodynamics ([80], [58] Ch 7, defined in [Eq. \(6\)](#)),

$$\begin{aligned} \log \tilde{\pi}_\beta^{(\text{geo})}(x) &= (1 - \beta) \log \tilde{\pi}_0(x) + \beta \log \tilde{\pi}_1(x) \\ \log_q \tilde{\pi}_\beta^{(q)}(x) &= (1 - \beta) \log_q \tilde{\pi}_0(x) + \beta \log_q \tilde{\pi}_1(x). \end{aligned} \quad (1)$$

Choosing a suitable path may facilitate more accurate MCMC estimators with fewer intermediate densities, as evidenced by experiments in [42, 54, 77].

---

### Algorithm 1: Annealed Importance Sampling

---

```

input : Endpoint densities  $\tilde{\pi}_0(x), \tilde{\pi}_1(x)$ 
        Schedule  $\{\beta_t\}_{t=0}^T$  and Annealing Path  $\beta_t \mapsto \tilde{\pi}_{\beta_t}(x)$ 
        Transition Kernels  $\mathcal{T}_t(x_t|x_{t-1})$  leaving  $\pi_{\beta_{t-1}}$  invariant

for  $k = 1$  to  $K$  do
   $x_0^{(k)} \sim \tilde{\pi}_0(x)$ ,  $w_0^{(k)} \leftarrow 1$ 
for  $t = 1$  to  $T$  do
  for  $k = 1$  to  $K$  do
     $x_t^{(k)} \sim \mathcal{T}_t(x_t^{(k)}|x_{t-1}^{(k)})$ ,  $w_t^{(k)} \leftarrow w_{t-1}^{(k)} \frac{\tilde{\pi}_{\beta_t}(x_t^{(k)})}{\tilde{\pi}_{\beta_{t-1}}(x_t^{(k)})}$ 
return Approximate samples:  $x_T \sim \pi_T(x)$ 
  Unbiased Estimator:  $\mathcal{Z}_T/\mathcal{Z}_0 = \mathbb{E}\left[\frac{1}{K} \sum_{k=1}^K w_T^{(k)}\right]$ 

```

---

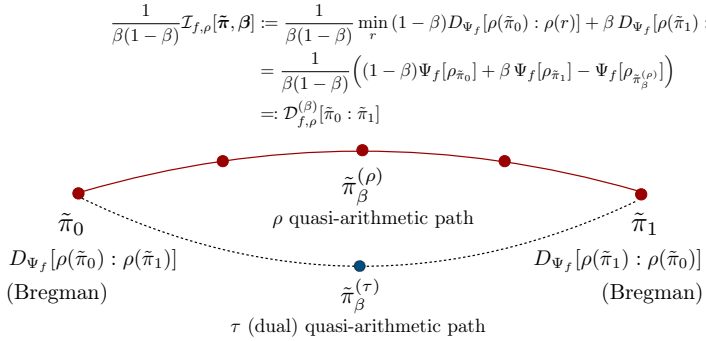


Fig. 1: Schematic illustrating our main results. The choice of a monotonic representation function  $\rho$ , along with either a convex function  $f$  or monotonic  $\tau$ , specifies a Bregman divergence for  $\beta = \{0, 1\}$ . The quasi-arithmetic path  $\tilde{\pi}_\beta^{(\rho)}$  with mixing weight  $\beta$  minimizes the expected Bregman divergence  $D_{\Psi_f}[\rho(\tilde{\pi}_a) : \rho(\tilde{\pi}_b)]$  to the endpoints  $\{\tilde{\pi}_0, \tilde{\pi}_1\}$ , where optimization is performed over the second argument and  $\Psi_f[\rho(\tilde{\pi})] := \int f(\rho(\tilde{\pi}(x))dx$ . The value of this objective associates a divergence  $D_{f,\rho}^{(\beta)}[\tilde{\pi}_0 : \tilde{\pi}_1]$  [86] (or scaled Bregman Information  $\frac{1}{\beta(1-\beta)} \mathcal{I}_{f,\rho}^{(\beta)}[\tilde{\pi}, \beta]$ ) with each intermediate density  $\tilde{\pi}_\beta^{(\rho)}$  along an annealing path between  $\tilde{\pi}_0$  and  $\tilde{\pi}_1$  (Example 2). Finally, the quasi-arithmetic path in the  $\rho$ -representation is a geodesic with respect to the primal connection induced by the Bregman divergence  $D_{\Psi_f}[\rho(\tilde{\pi}_a) : \rho(\tilde{\pi}_b)]$  for any  $\Psi_f$  (Thm. 2), with a similar interpretation for the  $\tau$ -representation and dual connection.

Intriguingly, Grosse et al. [42], Masrani et al. [54] show that densities along the paths in Eq. (1) minimize the expected divergence to the endpoints

$$\begin{aligned}
\tilde{\pi}_\beta^{(\text{geo})}(x) &= \arg \min_{\tilde{\pi}} (1-\beta) D_{\text{KL}}[\tilde{\pi} : \tilde{\pi}_0] + \beta D_{\text{KL}}[\tilde{\pi} : \tilde{\pi}_1] \\
\tilde{\pi}_\beta^{(q)}(x) &= \arg \min_{\tilde{\pi}} (1-\beta) D_A^{(\alpha)}[\tilde{\pi}_0 : \tilde{\pi}] + \beta D_A^{(\alpha)}[\tilde{\pi}_1 : \tilde{\pi}]
\end{aligned} \tag{2}$$

where  $D_A^{(\alpha)}$  indicates Amari's  $\alpha$ -divergence [4, 5, 6] using the reparameterization  $\alpha \leftarrow \frac{1+\hat{\alpha}}{2}$  with  $\alpha = q$ ,

$$D_A^{(\alpha)}[\tilde{\pi}_a : \tilde{\pi}_b] = \frac{1}{\alpha} \int \tilde{\pi}_a(x) dx + \frac{1}{1-\alpha} \int \tilde{\pi}_b(x) dx - \frac{1}{\alpha} \frac{1}{1-\alpha} \int \tilde{\pi}_a(x)^{1-\alpha} \tilde{\pi}_b(x)^\alpha dx. \tag{3}$$

The minimization in Eq. (2) is reminiscent of the problem of finding the 'centroid', or  $\arg \min_\mu \mathbb{E}_{\nu(u)} D[u : \mu]$ , of a random variable  $U \sim \nu$  with respect to a statistical divergence  $D$  and sampling measure  $\nu(u)$  [76, 67, 65]. While properties of this optimization depend on the choice of divergence in general, Banerjee et al. [10, 11] show that for *any* Bregman divergence, minimization in the second argument yields the arithmetic mean  $\mu^* = \mathbb{E}_\nu[u]$  as the unique optimal centroid. In fact, the property of the arithmetic mean as the centroid characterizes the Bregman divergences among divergences or loss functions

[10]. At this minimizing argument, the expected divergence in Eq. (2) reduces to a gap in Jensen’s inequality, known as the Bregman Information [11].

Our main result in Thm. 1 uses the rho-tau Bregman divergence framework of Zhang [86, 87] to extend the Bregman Information results of Banerjee et al. [11] to quasi-arithmetic means. A key observation is that the minimizing arguments in Eq. (1) are arithmetic means after applying a monotonic *representation function*  $\rho(\tilde{\pi}) = \log_q \tilde{\pi}$ . The Bregman Information further associates a divergence functional with each intermediate density along a  $q$ -path between  $\tilde{\pi}_0$  and  $\tilde{\pi}_1$  (Fig. 1), encompassing many common divergences as special cases (Table 1). Our analysis highlights the interplay between quasi-arithmetic means and divergence functionals, and naturally bridges between parametric [7] and nonparametric information geometry [87, 59]. Via the intuitive example of annealing paths, we seek to familiarize a wider machine learning audience with the referential-representational biduality in information geometry [86, 87].

While the foundation for many of the above results appears in Zhang [86, 87][89], our analysis emphasizes divergence minimization properties (Sec. 3) and parametric interpretations (Sec. 4.2) by connecting the Bregman Information and representational  $\alpha$ -divergence studied in [86]. In Thm. 2, we show that annealing paths derived from quasi-arithmetic means are geodesic curves with respect to the affine connections induced by rho-tau Bregman divergences. Finally, we provide novel variational representations of  $q$ -paths (Eq. (1), [54]) as the solution to an expected  $\beta$ -divergence [12, 33] or Cichocki-Amari  $(\alpha, \beta)$ -divergence [22] minimization in Sec. 4. Since MCMC applications consider unnormalized densities as input with the goal of calculating normalization constants, we discuss in Example 12 how our analysis differs from prior work involving quasi-arithmetic means of normalized densities [76, 5, 35, 84].

*Notation* Throughout this work, we consider a measure space  $(\mathcal{X}, \Sigma, dx)$ . We denote probability densities with respect to  $dx$  as  $\pi(x)$  and indicate unnormalized densities, which may not integrate to 1, using  $\tilde{\pi}(x)$ . All integrals  $\int(\cdot) dx$  are assumed to be over the domain  $\mathcal{X}$ .

## 2 Bregman Divergence under Monotonic Embedding

We begin by reviewing the notion of a quasi-arithmetic mean associated with a monotonic embedding function in Sec. 2.1, and describe how such embedding functions can be used to define divergence functionals in the rho-tau Bregman divergence framework of [86, 87, 59, 89] in Sec. 2.2.

### 2.1 Quasi-Arithmetic Means

Consider a strictly monotonic, continuously differentiable *representation function*  $\rho : \mathcal{X}_\rho \subset \mathbb{R} \rightarrow \mathcal{Y}_\rho \subset \mathbb{R}$ . Given a set of input elements  $\mathbf{u} = (u_1, \dots, u_N)$  with  $u_i \in \mathcal{X}_\rho$  and nonnegative mixing weights  $\boldsymbol{\beta} = (\beta_1, \dots, \beta_N)$  which are normalized  $\sum_{i=1}^N \beta_i = 1$ , the *quasi-arithmetic mean* [49] is

$$\mu_\rho(\mathbf{u}, \boldsymbol{\beta}) = \rho^{-1} \left( \sum_{i=1}^N \beta_i \cdot \rho(u_i) \right). \quad (4)$$

We will primarily focus on the setting where each input  $u_i = \tilde{\pi}_i(x)$  is a density function. Since the function  $\rho$  is monotonic and thus invertible, we may represent a given density  $\tilde{\pi}(x)$  using  $\rho(\tilde{\pi}(x))$  without loss of information. This is known as the  $\rho$ -*representation* of  $\tilde{\pi}$  [5, 6].

The property that  $\mu_\rho(\mathbf{u}, \boldsymbol{\beta})$  is  $\rho$ -affine, or linear in the  $\rho$ -representation of  $u_i$ 's [86], will play a key role in our later analysis. In other words,  $\mu_\rho(\mathbf{u}, \boldsymbol{\beta})$  is an arithmetic mean of the inputs after transformation by  $\rho(u)$

$$\rho(\mu_\rho(\mathbf{u}, \boldsymbol{\beta})) = \sum_{i=1}^N \beta_i \cdot \rho(u_i), \quad (5)$$

The quasi-arithmetic mean is also invariant to the affine transformations of  $\rho$ , with  $\mu_\rho(\mathbf{u}, \boldsymbol{\beta}) = \mu_{\rho_{c,a}}(\mathbf{u}, \boldsymbol{\beta})$  for  $\rho_{c,a}(u) = c\rho(u) + a$ ,  $c > 0$ , and  $a \in \mathbb{R}$ .

As a primary example of the representation function  $\rho$ , we will consider the family of  $q$ -deformed logarithms [80, 58] from nonextensive thermodynamics. For  $q, u > 0$ , the  $q$ -logarithm and its inverse, the  $q$ -exponential, are defined

$$\rho_q(u) := \log_q(u) = \frac{1}{1-q} (u^{1-q} - 1) \quad \exp_q(t) = [1 + (1-q)t]_+^{\frac{1}{1-q}}, \quad (6)$$

where  $[\cdot]_+ = \max(\cdot, 0)$ . While  $\log_q(u)$  is an affine transformation of the  $\alpha$ -representation [5] (for  $\alpha = 2q - 1$ ), we will use the parameter  $q$  to avoid later confusion as to the role of the parameter  $\alpha$  [86, 87]. It can be shown that  $\log_q(u)$  is concave and strictly increasing in  $u$  [58] while, taking the limiting behavior as  $q \rightarrow 1$ , we recover the natural logarithm  $\log(u)$  and standard exponential  $\exp(t)$  as its inverse. The more general family of  $\phi$ -deformed logarithms ([56, 58, 59], App. G), including the  $\kappa$ -logarithm of [47], might also be considered. Our main results apply for arbitrary monotonic representation functions  $\rho(u)$ .

## 2.2 Rho-Tau Bregman Divergence

The rho-tau Bregman divergence of Zhang [86, 87] provides an elegant framework for understanding the relationship between divergence functions and representations of probability densities under monotonic embedding, and will form the basis of our later analysis.

Consider  $\rho$  and  $\tau$  to be scalar functions which applied to an unnormalized density function  $\tilde{\pi}(x)$ , map  $\tilde{\pi}(x) \mapsto \rho(\tilde{\pi}(x))$ . We consider a proper, strictly convex, lower semi-continuous function  $f : \mathbb{R} \mapsto \mathbb{R}$  applied to  $\rho(\tilde{\pi}) \in \mathbb{R}$ , and define  $f^*$  to be its convex conjugate. Using the Fenchel-Moreau biconjugation theorem, we can express  $f$  or  $f^*$  via a conjugate optimization,

$$f^*(\tau) = \sup_{\rho} \rho \cdot \tau - f(\rho) \quad f(\rho) = \sup_{\tau} \rho \cdot \tau - f^*(\tau). \quad (7)$$

Solving for the optimizing arguments above suggests the conjugacy conditions,

$$\tau = f'(\rho) = ((f^*)')^{-1}(\rho) \quad \rho = (f^*)'(\tau) = (f')^{-1}(\tau). \quad (8)$$

Zhang [86, 87] refer to these choices of  $\rho$  and  $\tau$  as *conjugate representations* with respect to the convex function  $f$ , emphasizing that the choice of two of these functions  $(\rho, \tau)$  or  $(\rho, f)$  determines the third one. In fact, for any choice of  $\rho, \tau$ , it is possible to find an appropriate  $f$ , with  $f' = \tau \circ \rho^{-1}$  due to the fact that set of strictly monotonic functions form a group, where the group action is function composition [88]. Finally, note that monotonicity of  $\rho = (f^*)'(\tau)$  is guaranteed if  $f^*$  is strictly convex. We will indeed interpret  $\rho(\tilde{\pi})$  as the representation function for the quasi-arithmetic mean in [Sec. 4](#).

We consider using the convex functions  $f(\rho)$  or  $f^*(\tau)$  to generate *decomposable* Bregman divergences [86, 87], where the arguments are now expressed as the  $\rho(\tilde{\pi})$  or  $\tau(\tilde{\pi})$  representations of the input density functions. Restricting attention to  $\tilde{\pi}$  such that  $\int f(\rho(\tilde{\pi}(x)))dx < \infty$  and  $\int f^*(\tau(\tilde{\pi}(x)))dx < \infty$ , we consider the decomposable Bregman divergence

$$\begin{aligned} D_f[\rho(\tilde{\pi}_a) : \rho(\tilde{\pi}_b)] & \quad (9) \\ &= \int f(\rho(\tilde{\pi}_a(x))) - f(\rho(\tilde{\pi}_b(x))) - (\rho(\tilde{\pi}_a(x)) - \rho(\tilde{\pi}_b(x)))f'(\rho(\tilde{\pi}_b(x)))dx, \end{aligned}$$

We will use the notation  $f(\rho_{\tilde{\pi}}(x)) := f(\rho(\tilde{\pi}(x)))$  and  $f^*(\tau_{\tilde{\pi}}(x)) := f^*(\tau(\tilde{\pi}(x)))$  moving forward, as a shorthand which emphasizes that our convex dualities are with respect to the scalar output of the representation functions  $\rho$  and  $\tau$ .

Finally, we define the negative rho-tau entropy functionals from [59] as

$$\Psi_f[\rho_{\tilde{\pi}}] = \int f(\rho(\tilde{\pi}(x)))dx \quad \Psi_{f^*}^*[\tau_{\tilde{\pi}}] = \int f^*(\tau(\tilde{\pi}(x)))dx, \quad (10)$$

While we primarily work with the definition in [Eq. \(9\)](#), it might also be viewed as a functional Bregman divergence  $D_f[\rho(\tilde{\pi}_a) : \rho(\tilde{\pi}_b)] = \Psi_f[\rho_{\tilde{\pi}_a}] - \Psi_f[\rho_{\tilde{\pi}_b}] - \delta\Psi_f[\rho_{\tilde{\pi}_b}](\rho_{\tilde{\pi}_a} - \rho_{\tilde{\pi}_b})$ , where  $\delta\Psi_f$  indicates the Frechet derivative (see [36] Prop. 2.3). As a result, we will also refer to [Eq. \(10\)](#) as decomposable generators.

Using the conjugate function  $f^*(\tau)$  or the corresponding  $\Psi_{f^*}^*[\tau]$ , we can also derive a *dual* rho-tau Bregman divergence. Noting that  $\rho_{\tilde{\pi}_b}(x) = (f^*)'(\tau_{\tilde{\pi}_b})$ , the dual divergences can be shown to be equivalent up to ordering of the arguments. Using the conjugate relationships in [Eq. \(7\)](#) and underlining terms involved in simplification steps, we have

$$\begin{aligned} D_{f^*}[\tau(\tilde{\pi}_a) : \tau(\tilde{\pi}_b)] &= \int f^*(\tau_{\tilde{\pi}_a}(x)) - \underline{f^*(\tau_{\tilde{\pi}_b}(x))} - (\tau_{\tilde{\pi}_a}(x) - \tau_{\tilde{\pi}_b}(x))\rho_{\tilde{\pi}_b}(x)dx \\ &= \int \underline{f^*(\tau_{\tilde{\pi}_a}(x))} + \underline{f(\rho_{\tilde{\pi}_b}(x))} - \tau_{\tilde{\pi}_a}(x)\rho_{\tilde{\pi}_b}(x)dx \quad (11) \\ &= \int f(\rho_{\tilde{\pi}_b}(x)) - \underline{f(\rho_{\tilde{\pi}_a}(x))} - (\rho_{\tilde{\pi}_b}(x) - \rho_{\tilde{\pi}_a}(x))\tau_{\tilde{\pi}_a}(x)dx \\ &= D_f[\rho(\tilde{\pi}_b) : \rho(\tilde{\pi}_a)]. \end{aligned}$$

[Eq. \(11\)](#) is the canonical form of the rho-tau Bregman divergence ([7] 3.4), which we can write in a mixed parameterization using  $\Psi_f$  and  $\Psi_{f^*}^*$

$$D_{f,f^*}[\rho(\tilde{\pi}_a) : \tau(\tilde{\pi}_b)] = \Psi_f[\rho_{\tilde{\pi}_a}] + \Psi_{f^*}^*[\tau_{\tilde{\pi}_b}] - \int \rho_{\tilde{\pi}_a}(x)\tau_{\tilde{\pi}_b}(x)dx. \quad (12)$$

Constructing  $D_{f^*,f}[\tau(\tilde{\pi}_b) : \rho(\tilde{\pi}_a)]$  in a similar fashion, we note that the various divergences are related by

$$D_f[\rho(\tilde{\pi}_a) : \rho(\tilde{\pi}_b)] = D_{f,f^*}[\rho(\tilde{\pi}_a) : \tau(\tilde{\pi}_b)] = D_{f^*,f}[\tau(\tilde{\pi}_b) : \rho(\tilde{\pi}_a)] = D_{f^*}[\tau(\tilde{\pi}_b) : \tau(\tilde{\pi}_a)].$$

The canonical divergences  $D_{f,f^*}, D_{f^*,f}$  are analogous to the *Fenchel-Young* losses studied in [15, 53, 64], here using rho-tau negative entropy functionals. Finally, note that the family of  $f$ -divergences [24, 25, 3] is a special case of the (decomposable) rho-tau Bregman divergence (see App. D or [86] Sec. 3.5-3.6).

**Example 1 (Forward and Reverse KL Divergence)** Consider the following representations functions  $\rho, \tau$ , which are conjugate with respect to convex functions  $f(\rho), f^*(\tau)$ ,

$$\begin{aligned} \rho(\tilde{\pi}) &= \log \tilde{\pi} & f(\rho) &= \exp\{\rho\} - \rho - 1 & \Psi_f[\rho_{\tilde{\pi}}] &= - \int \log \tilde{\pi}(x) dx + \int \tilde{\pi}(x) dx - 1 \\ \tau(\tilde{\pi}) &= \tilde{\pi} & f^*(\tau) &= \tau \log \tau - \tau + 1 & \Psi_{f^*}^*[\tau_{\tilde{\pi}}] &= \int \tilde{\pi}(x) \log \tilde{\pi}(x) dx - \int \tilde{\pi}(x) dx + 1, \end{aligned}$$

where  $\Psi_{f^*}^*[\tau(\tilde{\pi})] = \Psi_{f^*}^*[\tilde{\pi}]$  is the negative Shannon entropy. Using these generators for the rho-tau Bregman divergence in Eq. (9), we recover the KL divergence with different orders of the arguments,

$$D_f[\rho(\tilde{\pi}_a) : \rho(\tilde{\pi}_b)] = D_{\text{KL}}[\tilde{\pi}_b : \tilde{\pi}_a] \quad D_{f^*}[\tau(\tilde{\pi}_a) : \tau(\tilde{\pi}_b)] = D_{\text{KL}}[\tilde{\pi}_a : \tilde{\pi}_b]. \quad (13)$$

where the KL divergence between unnormalized densities is defined as

$$D_{\text{KL}}[\tilde{\pi}_a : \tilde{\pi}_b] = \int \tilde{\pi}_a(x) \log \frac{\tilde{\pi}_a(x)}{\tilde{\pi}_b(x)} dx - \int \tilde{\pi}_a(x) dx + \int \tilde{\pi}_b(x) dx. \quad (14)$$

Our notation in Eq. (9)-(13) is suggestive, as treating the  $\rho$ -representation as input to the Bregman divergence will lead to our main result in Thm. 1.

### 3 Main Result

The well-known results of Banerjee et al. [10, 11] show that the family of Bregman divergences is characterized by the fact that the arithmetic mean over inputs minimizes the expected divergence to a representative ‘centroid’ in the second argument. In this section, we use the rho-tau Bregman divergence framework to extend this result to quasi-arithmetic means (Thm. 1, 3), which will clarify the variational interpretations of the annealing paths in Eq. (2) (see Sec. 4). We refer to the value of the expected divergence minimization as the rho-tau Bregman Information.

In the case of two unnormalized probability densities  $\tilde{\pi}_0$  and  $\tilde{\pi}_1$  as input, the rho-tau Bregman Information matches the representational  $\alpha$ -divergence of Zhang [86, 87], thereby associating a divergence functional to each quasi-arithmetic mean along an annealing path. Analyzing the statistical manifold structure induced by these divergences, we show in Thm. 2 that the quasi-arithmetic mean under a monotonic embedding function  $\rho$  traces a geodesic

with respect to the primal affine connection induced by the Bregman divergence  $D_f[\rho(\tilde{\pi}_a) : \rho(\tilde{\pi}_b)]$  for any choice of  $\tau$  or  $f$ .

To begin, we prove the following theorem showing that the quasi-arithmetic mixture of densities  $\tilde{\pi}_i$  minimizes the expected rho-tau Bregman divergence, in similar spirit to Prop. 1 in Banerjee et al. [11]. We specialize to the case of two unnormalized densities  $\tilde{\pi}_0, \tilde{\pi}_1$  as input in [Example 2](#) and [Sec. 4](#).

**Theorem 1 (Rho-Tau Bregman Information)** *Consider a monotonic representation function  $\rho : \mathcal{X}_\rho \subset \mathbb{R} \mapsto \mathcal{Y}_\rho \subset \mathbb{R}$  and a convex function  $f : \mathcal{Y}_\rho \rightarrow \mathbb{R}$ . Consider discrete mixture weights  $\beta = \{\beta_i\}_{i=1}^N$  over  $N$  inputs  $\pi(x) = \{\pi_i(x)\}_{i=1}^N$ ,  $\pi_i(x) \in \mathcal{X}_\rho$ , with  $\sum_i \beta_i = 1$ . Finally, assume the expected value  $\mu_\rho(\pi, \beta) := \sum_{i=1}^N \beta_i \rho(\tilde{\pi}_i(x)) \in \text{ri}(\mathcal{Y}_\rho)$  is in the relative interior of the range of  $\rho$  for all  $x \in \mathcal{X}$ . Then, we have the following results,*

(i) *For a given Bregman divergence  $D_f[\rho(\tilde{\pi}_a) : \rho(\tilde{\pi}_b)]$  with generator  $\Psi_f$ , the optimization*

$$\mathcal{I}_{f,\rho}(\tilde{\pi}, \beta) := \min_{\mu} \sum_{i=1}^N \beta_i D_f[\rho(\tilde{\pi}_i) : \rho(\mu)]. \quad (15)$$

*has a unique minimizer given by the quasi-arithmetic mean with representation function  $\rho(\tilde{\pi})$*

$$\mu_\rho^*(\tilde{\pi}, \beta) = \rho^{-1} \left( \sum_{i=1}^N \beta_i \rho(\tilde{\pi}_i) \right) = \arg \min_{\mu} \sum_{i=1}^N \beta_i D_f[\rho(\tilde{\pi}_i) : \rho(\mu)].$$

*The arithmetic mean is recovered for  $\rho(\tilde{\pi}_i) = \tilde{\pi}_i$  and any  $f$  [11].*

(ii) *At this minimizing argument, the value of the expected divergence in Eq. (15) is called the Rho-Tau Bregman Information and is equal to a gap in Jensen's inequality for the convex functional  $\Psi[\rho_{\tilde{\pi}}] = \int f(\rho_{\tilde{\pi}}(x)) dx$ , mixture weights  $\beta$ , and inputs  $\tilde{\pi}$ ,*

$$\mathcal{I}_{f,\rho}(\tilde{\pi}, \beta) = \sum_{i=1}^N \beta_i \Psi_f[\rho(\tilde{\pi}_i)] - \Psi_f[\rho(\mu_\rho^*)]. \quad (16)$$

(iii) *Using  $\mu \neq \mu_\rho^*(\tilde{\pi}, \beta)$  as the representative in Eq. (15), the suboptimality gap is a rho-tau Bregman divergence*

$$D_{f,f^*}[\rho(\mu_\rho^*) : \tau(\mu)] = \sum_{i=1}^N \beta_i D_f[\rho(\tilde{\pi}_i) : \rho(\mu)] - \mathcal{I}_{f,\rho}(\tilde{\pi}, \beta) \quad (17)$$

*where  $D_{f,f^*}[\rho(\mu^*) : \tau(\mu)] = D_f[\rho(\mu^*) : \rho(\mu)] = D_{f^*}[\tau(\mu) : \tau(\mu^*)]$ .*

See [App. B](#) for the proof. We now consider the case of  $N = 2$  with unnormalized densities  $\tilde{\pi} = \{\tilde{\pi}_0, \tilde{\pi}_1\}$  as input, which will be a main object of interest in [Sec. 4](#).

**Example 2 (Rho-Tau Bregman Information and Divergences)** Consider the expected rho-tau Bregman divergence minimization for a decomposable generator  $\Psi_f[\rho(\tilde{\pi})]$ , inputs  $\tilde{\pi} = \{\tilde{\pi}_0, \tilde{\pi}_1\}$ , and weights  $\beta = \{1 - \beta, \beta\}$ .

$$\begin{aligned} \mathcal{I}_{f,\rho}(\tilde{\pi}, \beta) &:= \min_{\tilde{\pi}} (1 - \beta) D_f[\rho(\tilde{\pi}_0) : \rho(\tilde{\pi})] + \beta D_f[\rho(\tilde{\pi}_1) : \rho(\tilde{\pi})] \\ &= (1 - \beta) \Psi_f[\rho(\tilde{\pi}_0)] + \beta \Psi_f[\rho(\tilde{\pi}_1)] - \Psi_f[\rho(\tilde{\pi}_\beta^{(\rho)})] \end{aligned} \quad (18)$$

where the optimizing argument is given by the quasi-arithmetic mean

$$\tilde{\pi}_\beta^{(\rho)}(x) := \rho^{-1} \left( (1 - \beta) \rho(\tilde{\pi}_0(x)) + \beta \rho(\tilde{\pi}_1(x)) \right). \quad (19)$$

Introducing scaling factors to induce limiting behavior for  $\beta \rightarrow \{0, 1\}$ , the rho-tau Bregman Information matches the representational  $\alpha$ -divergence  $D_{f,\rho}^{(\beta)}[\tilde{\pi}_0 : \tilde{\pi}_1]$  of Zhang [86, 87],

$$\begin{aligned} D_{f,\rho}^{(\beta)}[\tilde{\pi}_0 : \tilde{\pi}_1] &:= \frac{1}{\beta(1 - \beta)} \mathcal{I}_{f,\rho}(\tilde{\pi}, \beta) \\ &= \begin{cases} \frac{1}{\beta(1 - \beta)} \left( (1 - \beta) \Psi_f[\rho(\tilde{\pi}_0)] + \beta \Psi_f[\rho(\tilde{\pi}_1)] - \Psi_f[\rho(\tilde{\pi}_\beta^{(\rho)})] \right) & (\beta \neq 1) \\ D_f[\rho(\tilde{\pi}_1) : \rho(\tilde{\pi}_0)] = D_{f^*}[\tau(\tilde{\pi}_0) : \tau(\tilde{\pi}_1)] & (\beta \rightarrow 1) \\ D_{f^*}[\tau(\tilde{\pi}_1) : \tau(\tilde{\pi}_0)] = D_f[\rho(\tilde{\pi}_0) : \rho(\tilde{\pi}_1)] & (\beta \rightarrow 0) \end{cases} \end{aligned} \quad (20)$$

where  $\tilde{\pi}_\beta^{(\rho)}$  is the quasi-arithmetic mean in Eq. (19). Eq. (20) thus associates a divergence functional comparing  $\tilde{\pi}_0$  and  $\tilde{\pi}_1$  with each quasi-arithmetic mean with weight  $\beta$  and representation function  $\rho$ .

Following Zhang [86, 87], we emphasize the ‘referential duality’ in terms of the mixing parameter  $\beta$ , where it is clear that, for example,  $D_{f,\rho}^{(\beta)}[\tilde{\pi}_0 : \tilde{\pi}_1] = D_{f,\rho}^{(1-\beta)}[\tilde{\pi}_1 : \tilde{\pi}_0]$ . ‘Representational duality’ is expressed by the fact that the divergences in the  $\rho$  and  $\tau$  representations, respectively, are equivalent up to reordering of the arguments  $D_f[\rho(\tilde{\pi}_a) : \rho(\tilde{\pi}_b)] = D_{f^*}[\tau(\tilde{\pi}_b) : \tau(\tilde{\pi}_a)]$  [86, 87].

Using the well-known Eguchi relations [31, 32], Zhang [86, 87] analyze the statistical manifold structures  $(\mathcal{M}, g, \nabla, \nabla^*)$  induced by the representational  $\alpha$ -divergence in Eq. (20) on the space of unnormalized density functions  $\mathcal{M}$ . We review these results in App. E.2. In particular, we prove the following proposition in App. F, which identifies the  $\rho$ - and  $\tau$ -representations as a pair of affine coordinate systems for the dually flat geometry induced by the Bregman divergence  $D_f[\rho(\tilde{\pi}_a) : \rho(\tilde{\pi}_b)]$ .

**Theorem 2** (Geodesics for Rho-Tau Bregman Divergence) *The curve  $\gamma_t = \rho^{-1}((1 - t)\rho(\tilde{\pi}_0) + t\rho(\tilde{\pi}_1))$  (with time derivative  $\dot{\gamma}_t = \frac{d}{dt}\gamma_t$ ) is auto-parallel with respect to the primal affine connection  $\nabla^{(1)}$  induced by the rho-tau Bregman divergence  $D_f[\rho(\tilde{\pi}_a) : \rho(\tilde{\pi}_b)]$  for  $\beta = 1$ . In other words,*

the following geodesic equation holds

$$\nabla_{\dot{\gamma}_t}^{(1)} \dot{\gamma}_t = d_{\dot{\gamma}_t} \dot{\gamma}_t + (\dot{\gamma}_t)^2 \cdot \left( \frac{\rho''(\gamma_t)}{\rho'(\gamma_t)} \right) = 0. \quad (21)$$

The  $\rho$ -representation of the unnormalized density thus provides an affine coordinate system for the geometry induced by  $D_f[\rho(\tilde{\pi}_a) : \rho(\tilde{\pi}_b)]$ .

## 4 Annealing Paths and Divergence Minimization

Using the rho-tau Bregman Information framework from the previous section, we are now able to understand and extend the variational representations of MCMC paths from Grosse et al. [42], Masrani et al. [54].

- Following Thm. 1, we derive  $q$ -annealing paths [54] as an expected divergence minimization for *any* rho-tau Bregman divergence with  $\rho(\tilde{\pi}) = \log_q \tilde{\pi}$  in Sec. 4.1. For different choices of convex function  $f$ , we recover the Amari  $\alpha$ -divergence minimization interpretation from Masrani et al. [54] or novel interpretations in terms of minimizing the  $\beta$ -divergence or the  $(\alpha, \beta)$ -divergence from Cichocki and Amari [22][23].
- In addition to the above interpretation, where the Amari  $\alpha$ -divergence corresponds to a rho-tau Bregman divergence for  $\alpha = q$  and  $\beta = 1$ , we show that the  $\alpha$ -divergence may *also* arise from the choice of mixture parameter  $\beta$ . In particular, under geometric averaging with  $q = 1$  with  $\rho(\tilde{\pi}) = \log \tilde{\pi}$ , the Amari  $\alpha$ -divergence corresponds to the rho-tau Bregman Information with  $\alpha = \beta$  (Example 4).
- We provide a parametric interpretation of the rho-tau Bregman Information in Sec. 4.2, where the mixing weight  $\beta$  is the natural parameter for a deformed  $q$ -exponential family.

We summarize our examples in Table 1, and refer the reader to Masrani et al. [54] for an empirical study of  $q$ -paths for MCMC applications in Bayesian inference and marginal likelihood evaluation.

We begin by providing two common examples of the rho-tau Bregman Information corresponding to the arithmetic mixture and geometric mixture paths. First, recall the choices defining the forward and reverse KL divergences in Example 1,

$$\begin{aligned} \rho(\tilde{\pi}) &= \log \tilde{\pi} & f(\rho) &= \exp\{\rho\} - \rho - 1 \\ \tau(\tilde{\pi}) &= \tilde{\pi} & f^*(\tau) &= \tau \log \tau - \tau + 1 \end{aligned}$$

where the dual decomposable generator or rho-tau negative entropy  $\Psi_{f^*}^*[\tau(\tilde{\pi})]$  is a functional of the density directly, and matches the negative Shannon entropy

$$\Psi_{f^*}^*[\tilde{\pi}] = \int \tilde{\pi}(x) \log \tilde{\pi}(x) dx - \int \tilde{\pi}(x) dx + 1. \quad (22)$$

Familiar Divergences from scaled Bregman Information			
Convex Function	Bregman Divergence	Bregman Information	
	$\beta \rightarrow 0$	$\beta \rightarrow 1$	$\beta \notin \{0, 1\}$
$\log \mathcal{Z}_1(\beta) = \log \int \tilde{\pi}_\beta^{(\text{geo})}(x) dx$	$D_{\text{KL}}[\pi_0 : \pi_1]$	$D_{\text{KL}}[\pi_1 : \pi_0]$	$D_R^{(\beta)}[\pi_0 : \pi_1]$
$\mathcal{Z}_1(\beta) = \int \tilde{\pi}_\beta^{(\text{geo})}(x) dx$	$D_{\text{KL}}[\tilde{\pi}_0 : \tilde{\pi}_1]$	$D_{\text{KL}}[\tilde{\pi}_1 : \tilde{\pi}_0]$	$D_A^{(\beta)}[\tilde{\pi}_0 : \tilde{\pi}_1]$
$\mathcal{Z}_q(\beta) = \int \tilde{\pi}_\beta^{(q)}(x) dx$	$D_A^{(q)}[\tilde{\pi}_0 : \tilde{\pi}_1]$	$D_A^{(q)}[\tilde{\pi}_1 : \tilde{\pi}_0]$	$D_Z^{(\beta, q)}[\tilde{\pi}_0 : \tilde{\pi}_1]$
$\mathcal{Z}_0(\beta) = \int \tilde{\pi}_\beta^{(\text{arith})}(x) dx$	$D_{\text{KL}}[\tilde{\pi}_1 : \tilde{\pi}_0]$	$D_{\text{KL}}[\tilde{\pi}_0 : \tilde{\pi}_1]$	$D_{\text{JS}}^{(\beta)}[\tilde{\pi}_0 : \tilde{\pi}_1]$
$\Psi_f[\rho(\tilde{\pi}_\beta^{(q)})] = \int \tilde{\pi}_\beta^{(q)}(x)^{2-q} dx$	$D_B^{(2-q)}[\tilde{\pi}_1 : \tilde{\pi}_0]$	$D_B^{(2-q)}[\tilde{\pi}_0 : \tilde{\pi}_1]$	see Ex. 8
$\Psi_f[\rho(\tilde{\pi}_\beta^{(q)})] = \int \tilde{\pi}_\beta^{(q)}(x)^{\lambda+1-q} dx$	$D_C^{(q, \lambda)}[\tilde{\pi}_1 : \tilde{\pi}_0]$	$D_C^{(q, \lambda)}[\tilde{\pi}_0 : \tilde{\pi}_1]$	see Eq. (30)

Table 1: Bregman Information and Divergence Functionals. For a convex function  $\Psi_f[\rho]$  or  $\mathcal{Z}_q(\beta)$  (see Sec. 4.2), the Bregman Information is a gap in Jensen’s inequality (first line) obtained by minimizing the expected Bregman divergence as in Eq. (2). The scaled Bregman Information matches the representational  $\alpha$ -divergence  $D_{f, \rho}^{(\beta)}$  in [86] (Example 2). Note  $D_R^{(\alpha)}$  is Rényi’s  $\alpha$ -divergence,  $D_A^{(\alpha)}$  is Amari’s  $\alpha$ -divergence,  $D_{\text{JS}}^{(\alpha)}$  is the Jensen-Shannon divergence with mixture weight  $\alpha$ ,  $D_Z^{(\beta, q)}$  is the  $(\alpha, \beta)$  divergence of Zhang [86],  $D_B^{(q)}$  is the  $\beta$ -divergence of order  $q$  [12], and  $D_C^{(\lambda, q)}$  is the  $(\alpha, \beta)$  divergence of Cichocki and Amari [22].

### Example 3 (Jensen-Shannon Divergence as a Bregman Information)

The (weighted) Jensen-Shannon divergence (JSD) [19, 50] is the most natural example of a Bregman Information, with  $D_{\text{JS}}^{(\beta)}[\tilde{\pi}_0 : \tilde{\pi}_1] = \mathcal{I}_{f^*, \tau}(\tilde{\pi}, \beta)$  corresponding to the forward KL divergence in Example 1. First, recall the definition

$$D_{\text{JS}}^{(\beta)}[\tilde{\pi}_0 : \tilde{\pi}_1] := \int (1 - \beta) \tilde{\pi}_0(x) \log \frac{\tilde{\pi}_0(x)}{\pi_\beta^{(\text{arith})}(x)} dx + \beta \tilde{\pi}_1(x) \log \frac{\tilde{\pi}_1(x)}{\pi_\beta^{(\text{arith})}(x)} dx.$$

The arithmetic mixture  $\pi_\beta^{(\text{arith})}(x) := (1 - \beta)\tilde{\pi}_0(x) + \beta\tilde{\pi}_1(x)$  minimizes the expected divergence in the  $\tau(\tilde{\pi}) = \tilde{\pi}$  representation, which yields

$$\begin{aligned} \mathcal{I}_{f^*, \tau}(\tilde{\pi}, \beta) &= \min_{\tilde{\pi}} (1 - \beta) D_{f^*}[\tau(\tilde{\pi}_0) : \tau(\pi_\beta^{(\text{arith})})] + \beta D_{f^*}[\tau(\tilde{\pi}_1) : \tau(\pi_\beta^{(\text{arith})})] \\ &= (1 - \beta) D_{\text{KL}}[\tilde{\pi}_0 : \pi_\beta^{(\text{arith})}] + \beta D_{\text{KL}}[\tilde{\pi}_1 : \pi_\beta^{(\text{arith})}] \\ &= (1 - \beta) \Psi_{f^*}^*[\tilde{\pi}_0] + \beta \Psi_{f^*}^*[\tilde{\pi}_1] - \Psi_{f^*}^*[\pi_\beta^{(\text{arith})}], \end{aligned}$$

where  $\Psi_{f^*}^*[\tilde{\pi}]$  is the negative Shannon entropy as in Eq. (22).

**Example 4 (Geometric Path, with  $\alpha$ -Div. as Bregman Information)**

When minimizing the reverse KL divergence  $D_f[\rho(\tilde{\pi}_a) : \rho(\tilde{\pi}_b)] = D_{\text{KL}}[\tilde{\pi}_b : \tilde{\pi}_a]$ , note that optimizing over the second argument of the rho-tau Bregman divergence corresponds to optimizing over the first argument of the KL divergence. The geometric mixture, or quasi-arithmetic mean for  $\rho(\tilde{\pi}) = \log \tilde{\pi}$ ,

$$\tilde{\pi}_\beta^{(\text{geo})}(x) := \tilde{\pi}_0(x)^{1-\beta} \tilde{\pi}_1(x)^\beta = \arg \min_{\tilde{\pi}} (1-\beta) D_{\text{KL}}[\tilde{\pi} : \tilde{\pi}_0] + \beta D_{\text{KL}}[\tilde{\pi} : \tilde{\pi}_1],$$

provides the minimizing argument as in Grosse et al. [42]. After simplifying, the scaled Bregman Information recovers the Amari  $\alpha$ -divergence in Eq. (3),

$$\begin{aligned} & \frac{1}{\beta(1-\beta)} \mathcal{I}_{f,\rho}(\tilde{\pi}, \beta) \\ &= \frac{1}{\beta(1-\beta)} \left( (1-\beta) D_{\text{KL}}[\tilde{\pi}_\beta^{(\text{geo})} : \tilde{\pi}_0] + \beta D_{\text{KL}}[\tilde{\pi}_\beta^{(\text{geo})} : \tilde{\pi}_1] \right) \\ &= \frac{1}{\beta(1-\beta)} \left( (1-\beta) \Psi_f[\rho_{\tilde{\pi}_0}] + \beta \Psi_f[\rho_{\tilde{\pi}_1}] - \Psi_f[\rho_{\tilde{\pi}_\beta^{(\text{geo})}}] \right) \\ &= \frac{1}{\beta(1-\beta)} \left( (1-\beta) \int \tilde{\pi}_0(x) dx + \beta \int \tilde{\pi}_1(x) dx - \int \tilde{\pi}_0(x)^{1-\beta} \tilde{\pi}_1(x)^\beta dx \right) \\ &= D_A^{(\beta)}[\tilde{\pi}_0 : \tilde{\pi}_1]. \end{aligned} \tag{23}$$

Note that the order of the  $\alpha$ -divergence is set by the mixture parameter  $\beta$ , which is analogous to an inverse temperature parameter in maximum entropy or lossy compression applications [46, 78, 13, 2].

#### 4.1 $q$ -Paths from a Divergence Minimization Perspective

Following Thm. 1-2 and the examples above, the  $q$ -annealing paths from Maserani et al. [54], which correspond to a quasi-arithmetic mean of two endpoint unnormalized densities  $\tilde{\pi} = \{\tilde{\pi}_0, \tilde{\pi}_1\}$  with weight  $\beta$ , should arise from *any* rho-tau Bregman divergence in the  $\rho_q(\tilde{\pi}) = \log_q \tilde{\pi}$  representation,

$$\begin{aligned} \tilde{\pi}_\beta^{(q)}(x) &= \exp_q \{(1-\beta) \log_q \tilde{\pi}_0(x) + \beta \log_q \tilde{\pi}_1(x)\}, \\ &= \arg \min_{\tilde{\pi}} (1-\beta) D_f[\rho(\tilde{\pi}_0) : \rho(\tilde{\pi})] + \beta D_f[\rho(\tilde{\pi}_1) : \rho(\tilde{\pi})] \end{aligned} \tag{24}$$

The choice of convex function  $f$  or dual representation  $\tau$  is an additional degree of freedom in specifying the divergence, suggesting that the  $q$ -annealing path can be viewed as the Bregman centroid for a wide range of divergences.

In Sec. 4.1.1, we describe a family of rho-tau Bregman divergences corresponding to the  $(\alpha, \beta)$  divergence of Cichocki and Amari [22][23], which includes the Amari  $\alpha$ -divergence and Beta divergence as special cases. We derive the corresponding rho-tau Bregman Informations and divergence minimization interpretations of  $q$ -paths in Sec. 4.1.2.

#### 4.1.1 Rho-Tau Bregman Divergence

Consider the family of dual representations  $\tau(\tilde{\pi})$  defined by another deformed  $q$ -logarithm of order  $\lambda$ ,

$$\rho(\tilde{\pi}) = \log_q(\tilde{\pi}) = \frac{1}{1-q}\tilde{\pi}(x)^{1-q} - \frac{1}{1-q} \quad \tau(\tilde{\pi}) = \log_{1-\lambda}(\tilde{\pi}) = \frac{1}{\lambda}\tilde{\pi}(x)^\lambda - \frac{1}{\lambda}.$$

As in Sec. 2.2, the above  $\rho$  and  $\tau$  representations will be conjugate with respect to the convex function for which  $f' = \tau \circ \rho^{-1}$  (see Eq. (8)). Choosing an additive constant to induce limiting behavior as  $q \rightarrow 1$  or  $\lambda \rightarrow 0$  (see App. H), we write the convex function  $f$  and decomposable generator  $\Psi_f[\rho_{\tilde{\pi}}] = \int f(\rho(\tilde{\pi}(x)))dx$  as

$$f(\rho) = \frac{1}{\lambda} \frac{1}{\lambda + 1 - q} \exp_q\{\rho\}^{\lambda+1-q} - \frac{1}{\lambda}\rho - \frac{1}{\lambda(\lambda + 1 - q)}. \quad (25)$$

$$\Psi_f[\rho_{\tilde{\pi}}] = \frac{1}{\lambda} \frac{1}{\lambda + 1 - q} \int \tilde{\pi}(x)^{\lambda+1-q}dx - \frac{1}{\lambda} \frac{1}{1-q} \int \tilde{\pi}(x)^{1-q}dx - \frac{1}{\lambda(\lambda + 1 - q)}.$$

Finally, the rho-tau Bregman divergence  $D_f[\rho(\tilde{\pi}_a) : \rho(\tilde{\pi}_b)]$  corresponds to the  $(\alpha, \beta)$  divergence of Cichocki and Amari [22][23]

$$D_C^{(q, \lambda)}[\tilde{\pi}_a : \tilde{\pi}_b] := \frac{1}{\lambda(1-q)(\lambda + 1 - q)} \left( (1-q) \int \tilde{\pi}_a(x)^{\lambda+1-q}dx + \lambda \int \tilde{\pi}_b(x)^{\lambda+1-q}dx \right. \\ \left. - (\lambda + 1 - q) \int \tilde{\pi}_a(x)^\lambda \tilde{\pi}_b(x)^{1-q}dx \right). \quad (26)$$

#### Example 5 (Amari $\alpha$ -Divergence as Rho-Tau Bregman Divergence)

Choosing  $\lambda = q$ , the dual representation becomes the  $1-q$  logarithm  $\tau(\tilde{\pi}) = \log_{1-q}(\tilde{\pi}) = \frac{1}{q}\tilde{\pi}(x)^q - \frac{1}{q}$ , which is known as the  $\tau$ -deformed gauge in Naudts and Zhang [59]. Using the generator in Eq. (25), the Bregman divergence  $D_f[\rho(\tilde{\pi}_a) : \rho(\tilde{\pi}_b)]$  is the Amari  $\alpha$ -divergence

$$D_A^{(q)}[\tilde{\pi}_a : \tilde{\pi}_b] = \frac{1}{q} \int \tilde{\pi}_a(x)dx + \frac{1}{1-q} \int \tilde{\pi}_b(x)dx - \frac{1}{q} \frac{1}{1-q} \int \tilde{\pi}_a(x)^{1-q} \tilde{\pi}_b(x)^q dx$$

Note that, in contrast to Example 4, the Amari  $\alpha$ -divergence is a rho-tau Bregman divergence (instead of a Bregman Information), with the order set by the representation parameter  $q$  (instead of the mixing weight  $\beta$ ).

#### Example 6 (Beta-Divergence as Rho-Tau Bregman Divergence)

Choosing  $\lambda = 1$  and modifying the dual representation to be  $\tau(\tilde{\pi}) = \tilde{\pi}$ , we have the following choices of  $f$  and  $f^*$

$$\begin{aligned} \tau_{\tilde{\pi}}(x) &= \tilde{\pi}(x) & \rho_{\tilde{\pi}}(x) &= \log_q \tilde{\pi}(x). \\ f(\rho) &= \frac{1}{2-q} [1 + (1-q)\rho]_+^{\frac{2-q}{1-q}} - \frac{1}{2-q} & = \log_{q-1} (\exp_q\{\rho\}) \end{aligned} \quad (27)$$

which is known as the  $\tau$ -identity gauge in [59, 89]. The associated rho-tau Bregman divergence is the Beta-divergence ([12, 55, 33, 58] Ch. 8) matches Eq. (26) for  $\lambda = 1$ ,

$$\begin{aligned} D_B^{2-q}[\tilde{\pi}_b : \tilde{\pi}_a] &:= \frac{1}{1-q} \frac{1}{2-q} \int \tilde{\pi}_b(x)^{2-q} dx + \frac{1}{2-q} \int \tilde{\pi}_a(x)^{2-q} dx - \frac{1}{1-q} \int \tilde{\pi}_b(x) \tilde{\pi}_a(x)^{1-q} dx \\ &= D_f[\rho(\tilde{\pi}_a) : \rho(\tilde{\pi}_b)] \end{aligned} \quad (28)$$

where we note that the order of the arguments is reversed in  $D_B$  compared to  $D_f$ . We emphasize that the representation parameter  $q$  sets the order of the Beta divergence, rather than the mixing parameter  $\beta$ .

For the  $\tau$ -identity case, we call attention to the form of the dual generator

$$\begin{aligned} f^*(\tau) &= \frac{1}{1-q} \frac{1}{2-q} \tau^{2-q} - \frac{1}{1-q} \tau + \frac{1}{2-q} = \frac{1}{1-q} \log_{q-1}(\tau) - \frac{1}{1-q} \tau + \frac{1}{1-q}. \\ \Psi_{f^*}^*[\tilde{\pi}] &= \frac{1}{(1-q)(2-q)} \int \tilde{\pi}(x)^{2-q} dx - \int \frac{1}{1-q} \tilde{\pi}(x) dx + \frac{1}{2-q}. \end{aligned}$$

In particular, since  $\tau(\tilde{\pi}) = \tilde{\pi}$ , we can directly interpret the dual generator  $\Psi_{f^*}^*[\tilde{\pi}]$  as the negative Tsallis entropy functional of order  $2-q$  [79, 80, 58]. The Beta divergence thus corresponds to the Bregman divergence generated by the negative Tsallis entropy ([58] Sec. 8.7, compare with Example 1).<sup>1</sup>

#### 4.1.2 Rho-Tau Bregman Information

Using Thm. 1 with  $\rho(\tilde{\pi}) = \log_q(\tilde{\pi})$ , we conclude that the  $q$ -annealing path minimizes the expected Cichocki-Amari divergence for any choice of  $(q, \lambda)$ ,

$$\tilde{\pi}_\beta^{(q)}(x) = \arg \min_{\tilde{\pi}} (1-\beta) D_C^{(q,\lambda)}[\tilde{\pi}_0 : \tilde{\pi}] + \beta D_C^{(q,\lambda)}[\tilde{\pi}_1 : \tilde{\pi}], \quad (29)$$

Interpreting the Bregman Information as a gap in Jensen's inequality for the generator  $\Psi_f[\rho_{\tilde{\pi}}]$  of the Cichocki-Amari divergence in Eq. (25), we have

$$\begin{aligned} \mathcal{I}_{f,\rho}(\tilde{\pi}, \beta) &= (1-\beta)\Psi_f[\rho(\tilde{\pi}_0)] + \beta\Psi_f[\rho(\tilde{\pi}_1)] - \Psi_f[\rho(\tilde{\pi}_\beta)] \quad (30) \\ &= \frac{1}{\lambda(\lambda+1-q)} \left( (1-\beta) \int \tilde{\pi}_0(x)^{\lambda+1-q} dx + \beta \int \tilde{\pi}_1(x)^{\lambda+1-q} dx \right. \\ &\quad \left. - \int \tilde{\pi}_\beta^{(q)}(x)^{\lambda+1-q} dx \right), \end{aligned}$$

Since the Bregman divergence generated by Eq. (25) is invariant to additional terms which are affine in  $\rho$  [11], the rho-tau Bregman Information in Eq. (30) reduces to a gap in Jensen's inequality for a functional which integrates each

<sup>1</sup> The identity dual representation leads to favorable properties for divergence minimization under linear constraints. Csiszár [27] characterize Beta divergences as providing scale-invariant projection onto the set of positive measures satisfying expectation constraints. Naudts [58] Ch. 8 discuss related thermodynamic interpretations. Here, the Beta divergence is preferred in place of the  $\alpha$ -divergence, which induces *escort* expectations due to the deformed dual representation  $\tau(\tilde{\pi}) = \log_{1-q} \tilde{\pi} = \frac{1}{q} \tilde{\pi}(x)^q - \frac{1}{q}$  from Example 5 [58, 89].

density raised to the  $\lambda + 1 - q$  power. As in [Example 2](#), scaling the Bregman Information in [Eq. \(30\)](#) by  $\frac{1}{\beta(1-\beta)}$  suggests a further family of divergence functionals  $D_{f,\rho}^{(\beta)}[\tilde{\pi}_0 : \tilde{\pi}_1]$  for comparing  $\tilde{\pi}_0$  and  $\tilde{\pi}_1$ . We summarize the Eguchi relations for these divergences in [App. E.2](#).

**Example 7 (Bregman Information induced by Amari  $\alpha$ -Divergence)**

For  $\lambda = q$  and the Amari  $\alpha$ -divergence from [Example 5](#), we recover the divergence minimization interpretation from [Eq. \(24\)](#) and Masrani et al. [54]

$$\tilde{\pi}_\beta^{(q)}(x) = \arg \min_{\tilde{\pi}} (1 - \beta) D_A^{(q)}[\tilde{\pi}_0 : \tilde{\pi}] + \beta D_A^{(q)}[\tilde{\pi}_1 : \tilde{\pi}] \quad (31)$$

The  $(\alpha, \beta)$  divergence from Zhang [86, 87] arises as the corresponding scaled Bregman Information, where we rename the  $(\alpha, \beta)$  divergence as  $D_Z^{(\beta,q)}[\tilde{\pi}_0 : \tilde{\pi}_1]$  to clarify the role of each parameter.

$$\begin{aligned} D_Z^{(\beta,q)}[\tilde{\pi}_0 : \tilde{\pi}_1] &:= \frac{1}{\beta(1-\beta)} \frac{1}{q} \left( \int (1 - \beta) \tilde{\pi}_0(x) + \beta \tilde{\pi}_1(x) - \tilde{\pi}_\beta^{(q)}(x) dx \right) \quad (32) \\ &= \frac{1}{\beta(1-\beta)} \mathcal{I}_{f,\rho}(\tilde{\pi}, \beta). \end{aligned}$$

Since  $\lambda + 1 - q = 1$  for  $\lambda = q$ , the divergence measures the difference between a mixture of normalization constants and the normalization constant of a quasi-arithmetic mean. Note that  $D_Z^{(\beta,q)}$  is also an  $f$ -divergence using  $f^{(\beta,q)}(u) = \frac{1}{\beta(1-\beta)} \frac{1}{q} ((1-\beta) + \beta u - ((1-\beta) + \beta u^{1-q})^{\frac{1}{1-q}})$ , and is shown by Zhang [86] to be the unique family of measure-invariant divergences satisfying the homogeneity condition  $D[c\tilde{\pi}_a : c\tilde{\pi}_b] = cD[\tilde{\pi}_a : \tilde{\pi}_b]$  (see [43] pg. 68, [5]).

Interpretations for the dual representation  $\tau(\tilde{\pi}) = \log_{1-q}(\tilde{\pi})$  are analogous, with  $\frac{1}{\beta(1-\beta)} \mathcal{I}_{f^*,\tau}(\tilde{\pi}, \beta) = D_Z^{(\beta,1-q)}[\tilde{\pi}_0 : \tilde{\pi}_1]$ . Further identities can be derived using the referential-representational dualities described below [Example 2](#).

**Example 8 (Bregman Information induced by the Beta-Divergence)**

For  $\lambda = 1$ , the  $q$ -annealing path arises from the expected Beta-divergence minimization over the first argument of  $D_B^{2-q}$  or second argument of  $D_f$

$$\tilde{\pi}_\beta^{(q)}(x) = \arg \min_{\tilde{\pi}} (1 - \beta) D_B^{(2-q)}[\tilde{\pi} : \tilde{\pi}_0] + \beta D_B^{(2-q)}[\tilde{\pi} : \tilde{\pi}_1]. \quad (33)$$

The resulting Bregman Information is a Jensen gap for a functional which raises each density to the power  $2 - q$  and integrates,

$$\mathcal{I}_{f,\rho}(\tilde{\pi}, \beta) = \frac{1}{2-q} \left( (1 - \beta) \int \tilde{\pi}_0(x)^{2-q} dx + \beta \int \tilde{\pi}_1(x)^{2-q} dx - \int \tilde{\pi}_\beta^{(q)}(x)^{2-q} dx \right).$$

Finally, we note that the mixture path minimizes the expected dual divergence  $D_{f^*}[\tau(\tilde{\pi}_a) : \tau(\tilde{\pi}_b)]$ , where the resulting Bregman Information becomes

$$\mathcal{I}_{f^*,\tau}(\tilde{\pi}, \beta) = \frac{1}{1-q} \frac{1}{2-q} \left( (1 - \beta) \int \tilde{\pi}_0(x)^{2-q} dx + \beta \int \tilde{\pi}_1(x)^{2-q} dx - \int \pi_\beta^{(\text{arith})}(x)^{2-q} dx \right).$$

#### 4.2 Parametric Interpretations using $q$ -Exponential Family with Parameter $\beta$

In this section, we interpret  $q$ -paths between given endpoints  $\tilde{\pi} = \{\tilde{\pi}_0, \tilde{\pi}_1\}$  as a one-parameter deformed exponential family with natural parameter  $\beta$ , allowing us to highlight connections with Rényi's  $\alpha$ -divergence and the  $\alpha$ -mixture family [5, 84].

Our starting point is to observe that the  $q$ -path in [Eq. \(24\)](#) can be written as a one-dimensional deformed 'likelihood ratio exponential family' [54, 16], with  $\tilde{\pi}_0(x)$  as a base density, the  $q$ -log likelihood ratio  $T(x) = \log_q \frac{\tilde{\pi}_1(x)}{\tilde{\pi}_0(x)}$  as the sufficient statistic, and the mixing weight  $\beta$  as the natural parameter. Assuming that  $\tilde{\pi}_1$  is absolutely continuous with respect to  $\tilde{\pi}_0$ ,

$$\tilde{\pi}_\beta^{(q)}(x) = \tilde{\pi}_0(x) \exp_q \left\{ \beta \cdot \log_q \frac{\tilde{\pi}_1(x)}{\tilde{\pi}_0(x)} \right\}. \quad (34)$$

A key observation is that the density ratio  $\tilde{\pi}_\beta^{(q)}(x)/\tilde{\pi}_0(x)$  is  $\rho$ -affine in the  $\log_q$  representation  $\rho(\tilde{\pi}_\beta^{(q)}(x)/\tilde{\pi}_0(x)) = \beta \cdot T(x)$  which, for given endpoint densities  $\{\tilde{\pi}_0, \tilde{\pi}_1\}$ , links the parametric family to the quasi-arithmetic mean and a family of divergence functionals derived from the rho-tau Bregman Information.

We will consider the multiplicative normalization constant for the  $q$ -likelihood ratio family as the convex generating function,

$$\frac{1}{q} \mathcal{Z}_q(\beta) = \frac{1}{q} \int \tilde{\pi}_\beta^{(q)}(x) dx = \frac{1}{q} \int \tilde{\pi}_0(x) \exp_q \left\{ \beta \cdot \log_q \frac{\tilde{\pi}_1(x)}{\tilde{\pi}_0(x)} \right\} dx, \quad (35)$$

where for the geometric path, we recover  $\mathcal{Z}_1(\beta) = \int \tilde{\pi}_0(x)^{1-\beta} \tilde{\pi}_1(x)^\beta dx$ .

**Example 9 (Parametric View of the Geometric Path)** The Bregman divergence induced by  $\mathcal{Z}_1(\beta)$  yields the reverse KL divergence (see [App. C](#)),

$$D_{\mathcal{Z}_1}[\beta_a : \beta_b] = D_{\text{KL}}[\tilde{\pi}_{\beta_b}^{(\text{geo})} : \tilde{\pi}_{\beta_a}^{(\text{geo})}]. \quad (36)$$

Note that we consider the parameter  $\beta$  as the input to the Bregman divergence, so that the geometric averaging path in [Example 4](#) corresponds to a simple arithmetic mixture of the endpoints  $\mathbf{u} = \{0, 1\}$  with weights  $\boldsymbol{\beta} = \{1 - \beta, \beta\}$

$$\beta = (1 - \beta) \cdot 0 + \beta \cdot 1 = \arg \min_{\beta_r} (1 - \beta) D_{\mathcal{Z}_1}[0 : \beta_r] + \beta D_{\mathcal{Z}_1}[1 : \beta_r]. \quad (37)$$

At this minimizer, the scaled Bregman Information matches the Amari  $\alpha$ -divergence  $D_A^{(\beta)}[\tilde{\pi}_0 : \tilde{\pi}_1]$ , as in [Eq. \(23\)](#)

$$\begin{aligned} D_{f,\rho}^{(\beta)}[\tilde{\pi}_0 : \tilde{\pi}_1] &= \frac{1}{\beta(1-\beta)} \left( (1-\beta)\mathcal{Z}_1(0) + \beta\mathcal{Z}_1(1) - \mathcal{Z}_1(\beta) \right) = D_A^{(\beta)}[\tilde{\pi}_0 : \tilde{\pi}_1] \\ &= \frac{1}{\beta(1-\beta)} \left( (1-\beta) \int \tilde{\pi}_0(x) dx + \beta \int \tilde{\pi}_1(x) dx - \int \tilde{\pi}_0(x)^{1-\beta} \tilde{\pi}_1(x)^\beta dx \right) \end{aligned}$$

**Example 10 (Rényi  $\alpha$ -Divergence as Bregman Information for Geometric Path)** For the geometric averaging path, we find that there is no distinction between treating the inputs as normalized probability densities  $\pi = \{\pi_0, \pi_1\}$  instead of unnormalized  $\tilde{\pi}$  (see Example 12 for differences in the case of  $q$ -paths). In particular, treating the *log* partition function as the generating function and restricting input to *normalized* densities, we have

$$D_\psi[\beta_a : \beta_b] = D_{\text{KL}}[\pi_{\beta_b}^{(\text{geo})} : \pi_{\beta_a}^{(\text{geo})}] \quad \text{for } \psi(\beta) := \log \mathcal{Z}_1(\beta), \quad (38)$$

$$\beta = (1 - \beta) \cdot 0 + \beta \cdot 1 = \arg \min_{\beta_r} (1 - \beta) D_\psi[0 : \beta_r] + \beta D_\psi[1 : \beta_r]. \quad (39)$$

We recognize the resulting scaled Bregman Information as the Rényi divergence [75, 81] of order  $\beta$ ,<sup>2</sup>

$$\begin{aligned} D_{f,\rho}^{(\beta)}[\tilde{\pi}_0 : \tilde{\pi}_1] &= \frac{1}{\beta(1 - \beta)} \left( (1 - \beta)\psi(0) + \beta\psi(1) - \psi(\beta) \right) = \frac{-1}{\beta(1 - \beta)} \log \int \pi_0(x)^{1-\beta} \pi_1(x)^\beta dx. \\ &= D_R^{(\beta)}[\pi_0(x) : \pi_1(x)] \end{aligned} \quad (40)$$

which matches the result in Nielsen and Nock [66] that the Rényi divergence between normalized distributions in the same exponential family is proportional to a gap in Jensen's inequality.

**Example 11 (Parametric View of  $q$ -Paths and Zhang  $(\alpha, \beta)$  Divergence)** We can also interpret the Amari  $\alpha$ -divergence as the Bregman divergence generated by the scaled normalization constant in Eq. (35) (see App. C),

$$D_{\frac{1}{q}\mathcal{Z}_q}[\beta_a : \beta_b] = D_A^{(q)}[\tilde{\pi}_{\beta_a} : \tilde{\pi}_{\beta_b}] \quad (41)$$

The  $q$ -path intermediate density  $\tilde{\pi}_\beta^{(q)}(x)$ , represented by the arithmetic mixture of  $\mathbf{u} = \{0, 1\}$ , minimizes the expected divergence  $\beta = \arg \min_{\beta_r} (1 - \beta) D_{\frac{1}{q}\mathcal{Z}_q}[0 : \beta_r] + \beta D_{\frac{1}{q}\mathcal{Z}_q}[1 : \beta_r]$  as in Eq. (37). This further leads to a parametric interpretation of Zhang's  $(\alpha, \beta)$  divergence Eq. (32) as the Bregman Information,

$$D_Z^{(\beta,q)}[\tilde{\pi}_0 : \tilde{\pi}_1] := \frac{1}{\beta(1 - \beta)} \frac{1}{q} \left( \int (1 - \beta) \mathcal{Z}_q(0) + \beta \mathcal{Z}_q(1) - \mathcal{Z}_q(\beta) \right). \quad (42)$$

For arbitrary endpoint densities  $\tilde{\pi}_0, \tilde{\pi}_1$  satisfying absolutely continuity and integrability conditions, we can thus construct a rich family of divergence functionals using the deformed likelihood ratio exponential family.

**Example 12 (Annealing between Normalized Probability Densities)**

Quasi-arithmetic means in the  $q$ - or  $\alpha$ -representation have been studied extensively [75, 5, 34, 35, 84], often in the context of normalized probability densities. Similarly to our results, it has been shown that the quasi-arithmetic

<sup>2</sup> Note that we have changed the order of arguments in order to match our definition of the  $\alpha$ -divergence [86, 5, 6], and used constant factors to induce limiting behavior of  $D_{\text{KL}}[\pi_a : \pi_b]$  as  $\alpha \rightarrow 0$  and  $D_{\text{KL}}[\pi_b : \pi_a]$  as  $\alpha \rightarrow 1$ .

mean in the  $q$ -representation minimizes the expected Amari  $\alpha$ -divergence to a normalized density in the second argument [5].

However, we highlight that the quasi-arithmetic mean of normalized  $\boldsymbol{\pi} = \{\pi_0, \pi_1\}$  or unnormalized densities  $\boldsymbol{\pi} = \{\tilde{\pi}_0, \tilde{\pi}_1\}$  *do not match* in the case of  $\rho(u) = \log_q u$ . For normalized inputs, the quasi-arithmetic mean  $\bar{\pi}_\beta^{(q)}$  becomes

$$\bar{\pi}_\beta^{(q)}(x) = \frac{1}{\bar{\mathcal{Z}}_q(\beta)} \pi_0(x) \exp_q \left\{ \beta \cdot \log_q \frac{\pi_1(x)}{\pi_0(x)} \right\} \quad (43)$$

$$= \frac{1}{c \cdot \bar{\mathcal{Z}}_q(\beta)} \tilde{\pi}_0(x) \exp_q \left\{ \frac{\beta \mathcal{Z}(1)^{q-1}}{(1-\beta)\mathcal{Z}(0)^{q-1} + \beta \mathcal{Z}(1)^{q-1}} \log_q \frac{\tilde{\pi}_1(x)}{\tilde{\pi}_0(x)} \right\} \quad (44)$$

where  $\mathcal{Z}(0)$  and  $\mathcal{Z}(1)$  are the normalization constants for  $\tilde{\pi}_0$  and  $\tilde{\pi}_1$ . Moving from [Eq. \(43\)](#) to [Eq. \(44\)](#) also requires dividing by  $c = [(1-\beta)\mathcal{Z}(0)^{-(1-q)} + \beta \mathcal{Z}(1)^{-(1-q)}]^{1-q}$ , which is a quasi-arithmetic mean of  $\mathcal{Z}^{-1}$  at the endpoints.

From [Eq. \(44\)](#), we observe that the  $q$ -mixture of normalized distributions,  $\bar{\pi}_\beta^{(q)}(x)$ , does not directly coincide with the  $\alpha$ -mixture of unnormalized endpoints,  $\pi_\beta^{(q)}(x) \propto \tilde{\pi}_\beta^{(q)}(x)$ . Instead, we need to adjust the mixing weight  $\beta' = \frac{\beta \mathcal{Z}(1)^{q-1}}{(1-\beta)\mathcal{Z}(0)^{q-1} + \beta \mathcal{Z}(1)^{q-1}}$  to obtain  $\bar{\pi}_\beta^{(q)}(x) = \pi_{\beta'}^{(q)}(x) \propto \tilde{\pi}_{\beta'}^{(q)}(x)$ . A similar time-reparameterization appears in Wong and Zhang [84], which interprets the normalized  $q$ -exponential family in terms of a deformation of the standard convex duality. This reparameterization of the mixing parameter  $\beta$  is usually intractable to calculate explicitly due to need to calculate normalization constants  $\mathcal{Z}(0)$ ,  $\mathcal{Z}(1)$ . By contrast, for the geometric path ( $q = 1$ ) in [Example 4](#) or [Example 9-10](#), the mixing parameter is the same for annealing between unnormalized and normalized endpoints.

**Example 13 (Moment-Averaging Path of Grosse et al. [42])** Finally, consider the special case of constructing an annealing path between two (normalized) endpoints  $\pi_{\boldsymbol{\theta}_0}$  and  $\pi_{\boldsymbol{\theta}_1}$  within an exponential family with sufficient statistics  $\mathbf{T}(x) = \{T^i(x)\}_{i=1}^d$ . In this case, we can recover the moment-averaging path of Grosse et al. [42] as a quasi-arithmetic mean  $\boldsymbol{\theta}_\beta = \boldsymbol{\eta}^{-1}((1-\beta)\boldsymbol{\eta}(\boldsymbol{\theta}_0) + \beta\boldsymbol{\eta}(\boldsymbol{\theta}_1))$  using the expectation parameter mapping  $\boldsymbol{\rho}(\boldsymbol{\theta}) = \boldsymbol{\eta}(\boldsymbol{\theta}) = \mathbb{E}_{\pi_{\boldsymbol{\theta}}}[\mathbf{T}(x)]$ . See [App. C.1](#) for details.

**Example 14 (Annealing within (Deformed) Exponential Families)** While we constructed one-dimensional deformed exponential families from arbitrary endpoint densities in [Eq. \(34\)](#) and [Example 9-11](#), the  $\rho$ -affine property of deformed exponential families yields a similar simplification for the special case of endpoints  $\tilde{\pi}_{\boldsymbol{\theta}_0}^{(q)}, \tilde{\pi}_{\boldsymbol{\theta}_1}^{(q)}$  which belong to the same parametric family. In particular, for the  $\rho(\tilde{\pi}) = \log_q \tilde{\pi}$  path within the  $\exp_q$  family, we have

$$\boldsymbol{\theta}_\beta = (1-\beta)\boldsymbol{\theta}_0 + \beta\boldsymbol{\theta}_1 = \arg \min_{\boldsymbol{\theta}_r} (1-\beta)D_{\frac{1}{q}\mathcal{Z}_q}[\boldsymbol{\theta}_0 : \boldsymbol{\theta}_r] + \beta D_{\frac{1}{q}\mathcal{Z}_q}[\boldsymbol{\theta}_1 : \boldsymbol{\theta}_r],$$

where  $D_{\frac{1}{q}\mathcal{Z}_q} = D_A^{(q)}$  is the Amari  $\alpha$ -divergence as in [Eq. \(41\)](#) and the KL divergence or exponential family case is recovered for  $q = 1$ . See [App. C](#) and [Example 15](#) for detailed discussion.

## 5 Conclusion and Discussion

In this work, we have generalized the Bregman divergence ‘centroid’ results of Banerjee et al. [11] to arbitrary monotonic embedding functions and quasi-arithmetic means. We identified annealing paths from the MCMC literature [60, 42, 54] as a natural setting where such quasi-arithmetic means appear. In particular, for two unnormalized density functions as input, we related the rho-tau Bregman divergence framework [86, 87, 59] to the Bregman Information from [11], and highlighted how various divergence functionals comparing  $\tilde{\pi}_0$  and  $\tilde{\pi}_1$  are associated with intermediate densities  $\tilde{\pi}_\beta$  along an annealing path.

We have seen that Amari’s  $\alpha$ -divergence arises via two different approaches. For the geometric averaging path ( $q = 1$ ), the  $\alpha$ -divergence appears as a Bregman Information with its order set by the mixture parameter  $\beta$  (Example 4). For the  $q$ -path, the  $\alpha$ -divergence appears as a rho-tau Bregman divergence with order set by the deformation parameter  $q$  (Example 5). In both cases, we provided parametric interpretations involving the Bregman divergence generated by the multiplicative normalization constant  $Z_q(\beta)$  of a one-dimensional (deformed) likelihood ratio exponential family.

However, for the geometric path, we also constructed a Bregman divergence using the *log* partition function of the one-dimensional exponential family  $\log Z(\beta)$ , where the corresponding scaled Bregman Information recovers the Rényi divergence as the gap in Jensen’s inequality for  $\psi(\beta)$  [66]. This derivation in terms of the mixing parameter  $\alpha = \beta$  is distinct from the approach of Wong and Zhang [84], where the Rényi divergence arises using the deformation parameter  $\alpha = q$ , the potential function  $\log Z_q(\beta)$ , and deformed *c*-duality. Further understanding the relationship between these constructions in terms of the  $\beta$  and  $q$  parameters remains an interesting question for future work.

Moving beyond the ubiquitous use of the KL divergence in machine learning, it would be interesting to further explore the use of rho-tau divergences in applications such as variational inference [48], constructing prediction losses [15, 8], and regularized reinforcement learning [37]. Clustering approaches based on quasi-arithmetic means have been proposed in [85, 82], and our insights might be used to develop probabilistic interpretations or algorithms similar to the original clustering motivations of the Bregman Information in [11]. Finally, future work might consider annealing paths based on the  $\phi$ -deformed logarithm (see App. G), or investigate ways to adaptively choose or learn a suitable path [77] or annealing schedule [40] based on statistics of a given sampling problem.

## References

1. Adlam B, Gupta N, Mariet Z, Smith J (2022) Understanding the bias-variance tradeoff of bregman divergences. arXiv preprint arXiv:220204167
2. Alemi A, Poole B, Fischer I, Dillon J, Saurous RA, Murphy K (2018) Fixing a Broken ELBO. In: International Conference on Machine Learning, pp 159–168
3. Ali SM, Silvey SD (1966) A general class of coefficients of divergence of one distribution from another. *Journal of the Royal Statistical Society: Series B (Methodological)* 28(1):131–142
4. Amari Si (1982) Differential geometry of curved exponential families-curvatures and information loss. *The Annals of Statistics* pp 357–385
5. Amari Si (2007) Integration of stochastic models by minimizing  $\alpha$ -divergence. *Neural computation* 19(10):2780–2796
6. Amari Si (2016) *Information geometry and its applications*, vol 194. Springer
7. Amari Si, Nagaoka H (2000) *Methods of information geometry*, vol 191. American Mathematical Soc.
8. Amid E, Anil R, Fifty C, Warmuth MK (2022) Layerwise bregman representation learning of neural networks with applications to knowledge distillation. *Transactions on Machine Learning Research*
9. Amos B, Xu L, Kolter JZ (2017) Input convex neural networks. In: International Conference on Machine Learning, PMLR, pp 146–155
10. Banerjee A, Guo X, Wang H (2005) On the optimality of conditional expectation as a Bregman predictor. *IEEE Transactions on Information Theory* 51(7):2664–2669
11. Banerjee A, Merugu S, Dhillon IS, Ghosh J (2005) Clustering with Bregman Divergences. *Journal of Machine Learning Research* 6:1705–1749
12. Basu A, Harris IR, Hjort NL, Jones M (1998) Robust and efficient estimation by minimising a density power divergence. *Biometrika* 85(3):549–559
13. Bercher JF (2012) A simple probabilistic construction yielding generalized entropies and divergences, escort distributions and  $q$ -Gaussians. *Physica A: Statistical Mechanics and its Applications* 391(19):4460–4469
14. Betancourt M, Byrne S, Livingstone S, Girolami M, et al. (2017) Geometric foundations of Hamiltonian Monte Carlo. *Bernoulli* 23(4A):2257–2298
15. Blondel M, Martins AF, Niculae V (2020) Learning with Fenchel-Young losses. *J Mach Learn Res* 21(35):1–69
16. Brekelmans R, Nielsen F, Galstyan A, Steeg GV (2020) Likelihood Ratio Exponential Families. In: NeurIPS Workshop on Information Geometry in Deep Learning, URL <https://openreview.net/forum?id=RoTADibt26>
17. Brekelmans R, Huang S, Ghassemi M, Steeg GV, Grosse RB, Makhzani A (2022) Improving Mutual Information Estimation with Annealed and Energy-Based Bounds. In: International Conference on Learning Representations
18. Buja A, Stuetzle W, Shen Y (2005) Loss functions for binary class probability estimation and classification: Structure and applications

19. Burbea J, Rao C (1982) Entropy differential metric, distance and divergence measures in probability spaces: A unified approach. *Journal of Multivariate Analysis* 12(4):575–596, DOI [https://doi.org/10.1016/0047-259X\(82\)90065-3](https://doi.org/10.1016/0047-259X(82)90065-3)
20. Chatterjee S, Diaconis P (2018) The sample size required in importance sampling. *The Annals of Applied Probability* 28(2):1099–1135
21. Chentsov N (1982) Statistical Decision Rules and Optimal Inference. *Translations of Mathematical Monographs* 53
22. Cichocki A, Amari Si (2010) Families of alpha-beta-and gamma-divergences: Flexible and robust measures of similarities. *Entropy* 12(6):1532–1568
23. Cichocki A, Cruces S, Amari Si (2011) Generalized alpha-beta divergences and their application to robust nonnegative matrix factorization. *Entropy* 13(1):134–170
24. Csiszár I (1964) Eine informationstheoretische ungleichung und ihre anwendung auf beweis der ergodizitaet von markoffschen ketten. *Magyer Tud Akad Mat Kutato Int Koezl* 8:85–108
25. Csiszár I (1967) Information-type measures of difference of probability distributions and indirect observation. *studia scientiarum Mathematicarum Hungarica* 2:229–318
26. Csiszár I (1967) Information-type measures of difference of probability distributions and indirect observation. *studia scientiarum Mathematicarum Hungarica* 2:229–318
27. Csiszár I (1991) Why least squares and maximum entropy? An axiomatic approach to inference for linear inverse problems. *The annals of statistics* 19(4):2032–2066
28. Del Moral P, Doucet A, Jasra A (2006) Sequential monte carlo samplers. *Journal of the Royal Statistical Society: Series B (Statistical Methodology)* 68(3):411–436
29. Duane S, Kennedy AD, Pendleton BJ, Roweth D (1987) Hybrid Monte Carlo. *Physics letters B* 195(2):216–222
30. Earl DJ, Deem MW (2005) Parallel tempering: Theory, applications, and new perspectives. *Physical Chemistry Chemical Physics* 7(23):3910–3916
31. Eguchi S (1983) Second order efficiency of minimum contrast estimators in a curved exponential family. *The Annals of Statistics* pp 793–803
32. Eguchi S (1985) A differential geometric approach to statistical inference on the basis of contrast functionals. *Hiroshima mathematical journal* 15(2):341–391
33. Eguchi S (2006) Information geometry and statistical pattern recognition. *Sugaku Expositions* 19(2):197–216
34. Eguchi S, Komori O (2015) Path connectedness on a space of probability density functions. In: *International Conference on Geometric Science of Information*, Springer, pp 615–624
35. Eguchi S, Komori O, Ohara A (2016) Information geometry associated with generalized means. In: *Information Geometry and its Applications IV*, Springer, pp 279–295

36. Frigyik BA, Srivastava S, Gupta MR (2008) Functional bregman divergence and bayesian estimation of distributions. *IEEE Transactions on Information Theory* 54(11):5130–5139
37. Geist M, Scherrer B, Pietquin O (2019) A theory of regularized Markov decision processes. In: International Conference on Machine Learning, PMLR, pp 2160–2169
38. Gelman A, Meng XL (1998) Simulating normalizing constants: From importance sampling to bridge sampling to path sampling. *Statistical science* pp 163–185
39. Gibilisco P, Pistone G (1998) Connections on non-parametric statistical manifolds by Orlicz space geometry. *Infinite Dimensional Analysis, Quantum Probability and Related Topics* 1(02):325–347
40. Goshtasbpour S, Cohen V, Perez-Cruz F (2023) Adaptive annealed importance sampling with constant rate progress. International Conference on Machine Learning
41. Grasselli MR (2010) Dual connections in nonparametric classical information geometry. *Annals of the Institute of Statistical Mathematics* 62(5):873–896
42. Grosse RB, Maddison CJ, Salakhutdinov RR (2013) Annealing between distributions by averaging moments. In: Advances in Neural Information Processing Systems, pp 2769–2777
43. Hardy G, Littlewood J, Pólya G (1953) Inequalities. *The Mathematical Gazette* 37(321):236–236
44. Jarzynski C (1997) Equilibrium free-energy differences from nonequilibrium measurements: A master-equation approach. *Physical Review E* 56(5):5018
45. Jarzynski C (1997) Nonequilibrium equality for free energy differences. *Physical Review Letters* 78(14):2690
46. Jaynes ET (1957) Information theory and statistical mechanics. *Physical review* 106(4):620
47. Kaniadakis G, Scarfone A (2002) A new one-parameter deformation of the exponential function. *Physica A: Statistical Mechanics and its Applications* 305(1-2):69–75
48. Knoblauch J, Jewson J, Damoulas T (2019) Generalized variational inference: Three arguments for deriving new posteriors. *arXiv preprint arXiv:190402063*
49. Kolmogorov AN (1930) Sur la notion de la moyenne. G. Bardi, tip. della R. Accad. dei Lincei
50. Lin J (1991) Divergence measures based on the Shannon entropy. *IEEE Transactions on Information theory* 37(1):145–151
51. Loaiza GI, Quiceno H (2013) A  $q$ -exponential statistical Banach manifold. *Journal of Mathematical Analysis and Applications* 398(2):466–476
52. Loaiza GI, Quiceno HR (2013) A Riemannian geometry in the  $q$ -Exponential Banach manifold induced by  $q$ -Divergences. In: Geometric Science of Information. First International Conference, GSI 2013, Paris, France, August 28-30, 2013. Proceedings, pp 737-742, Springer Berlin Hei-

delberg

53. Martins AF, Treviso M, Farinhas A, Aguiar PM, Figueiredo MA, Blondel M, Niculae V (2021) Sparse continuous distributions and fenchel-young losses. arXiv preprint arXiv:210801988
54. Masrani V, Brekelmans R, Bui T, Nielsen F, Galstyan A, Steeg GV, Wood F (2021) q-Paths: Generalizing the Geometric Annealing Path using Power Means. Uncertainty in Artificial Intelligence
55. Murata N, Takenouchi T, Kanamori T, Eguchi S (2004) Information geometry of U-Boost and Bregman divergence. *Neural Computation* 16(7):1437–1481
56. Naudts J (2004) Estimators, escort probabilities, and phi-exponential families in statistical physics. arXiv preprint math-ph/0402005
57. Naudts J (2009) The q-exponential family in statistical physics. *Open Physics* 7(3):405–413
58. Naudts J (2011) Generalised thermostatistics. Springer Science & Business Media
59. Naudts J, Zhang J (2018) Rho–tau embedding and gauge freedom in information geometry. *Information geometry* 1(1):79–115
60. Neal RM (2001) Annealed importance sampling. *Statistics and computing* 11(2):125–139
61. Neal RM (2011) MCMC Using Hamiltonian Dynamics. *Handbook of Markov Chain Monte Carlo* p 113
62. Nguyen X, Wainwright MJ, Jordan MI (2010) Estimating divergence functionals and the likelihood ratio by convex risk minimization. *IEEE Transactions on Information Theory* 56(11):5847–5861
63. Nielsen F (2020) An elementary introduction to information geometry. *Entropy* 22(10)
64. Nielsen F (2022) Statistical Divergences between Densities of Truncated Exponential Families with Nested Supports: Duo Bregman and Duo Jensen Divergences. *Entropy* 24(3):421
65. Nielsen F, Boltz S (2011) The burbea-rao and bhattacharyya centroids. *IEEE Transactions on Information Theory* 57(8):5455–5466
66. Nielsen F, Nock R (2011) On Rényi and Tsallis entropies and divergences for exponential families. arXiv preprint arXiv:11053259
67. Nock R, Nielsen F (2005) Fitting the smallest enclosing bregman ball. In: European Conference on Machine Learning, Springer, pp 649–656
68. Nock R, Cranko Z, Menon AK, Qu L, Williamson RC (2017) *f*-GANs in an information geometric nutshell. *Advances in Neural Information Processing Systems*
69. Nowozin S, Cseke B, Tomioka R (2016) *f*-GAN: Training generative neural samplers using variational divergence minimization. *Advances in neural information processing systems* 29
70. Ogata Y (1989) A Monte Carlo method for high dimensional integration. *Numerische Mathematik* 55(2):137–157
71. Pfau D (2013) A generalized bias-variance decomposition for Bregman divergences. Unpublished Manuscript

72. Pistone G, Sempi C (1995) An infinite-dimensional geometric structure on the space of all the probability measures equivalent to a given one. *The annals of statistics* pp 1543–1561
73. Poole B, Ozair S, Van Den Oord A, Alemi A, Tucker G (2019) On Variational Bounds of Mutual Information. In: International Conference on Machine Learning, pp 5171–5180
74. Rossky PJ, Doll J, Friedman H (1978) Brownian dynamics as smart Monte Carlo simulation. *The Journal of Chemical Physics* 69(10):4628–4633
75. Rényi A (1961) On Measures of Entropy and Information. In: Proceedings of the Fourth Berkeley Symposium on Mathematical Statistics and Probability, Berkeley, Calif., pp 547–561, URL <https://projecteuclid.org/euclid.bsmsp/1200512181>
76. Sibson R (1969) Information radius. *Zeitschrift für Wahrscheinlichkeitstheorie und verwandte Gebiete* 14(2):149–160
77. Syed S, Romaniello V, Campbell T, Bouchard-Côté A (2021) Parallel Tempering on Optimized Paths. International Conference on Machine Learning
78. Tishby N, Pereira FC, Bialek W (1999) The information bottleneck method. In: Proc. 37th Annual Allerton Conference on Communications, Control and Computing, 1999, pp 368–377
79. Tsallis C (1988) Possible generalization of Boltzmann-Gibbs statistics. *Journal of statistical physics* 52(1-2):479–487
80. Tsallis C (2009) Introduction to nonextensive statistical mechanics: approaching a complex world. Springer Science & Business Media
81. Van Erven T, Harremos P (2014) Rényi divergence and Kullback-Leibler divergence. *IEEE Transactions on Information Theory* 60(7):3797–3820
82. Vellal A, Chakraborty S, Xu JQ (2022) Bregman power k-means for clustering exponential family data. In: International Conference on Machine Learning, PMLR, pp 22103–22119
83. Welling M, Teh YW (2011) Bayesian learning via stochastic gradient Langevin dynamics. In: Proceedings of the 28th international conference on machine learning (ICML-11), Citeseer, pp 681–688
84. Wong TKL, Zhang J (2021) Tsallis and Rényi deformations linked via a new  $\lambda$ -duality. arXiv preprint arXiv:210711925
85. Xu J, Lange K (2019) Power k-means clustering. In: International conference on machine learning, PMLR, pp 6921–6931
86. Zhang J (2004) Divergence function, duality, and convex analysis. *Neural computation* 16(1):159–195
87. Zhang J (2013) Nonparametric information geometry: From divergence function to referential-representational biduality on statistical manifolds. *Entropy* 15(12):5384–5418
88. Zhang J (2015) On monotone embedding in information geometry. *Entropy* 17(7):4485–4499
89. Zhang J, Matsuzoe H (2021) Entropy, cross-entropy, relative entropy: Deformation theory (a). *Europhysics Letters* 134(1):18001

**Summary of Appendix** In App. A, we review annealed importance sampling as an example MCMC technique. In App. B, we prove our main result (Thm. 1). We discuss parameteric Bregman divergences and annealing paths between deformed exponential families from our representational perspective in App. C, where the  $\rho$ -affine property plays a crucial role. We interpret the family of  $f$ -divergences in our framework in App. D, which highlights a relationship between the Beta and  $\alpha$ -divergences. In App. E, we review the Eguchi relations and information-geometric structures induced by divergence functionals (see Table 2), and in App. F prove Thm. 2 showing that quasi-arithmetic paths in the  $\rho$ -representation are geodesics with respect to affine connections induced by the representational Bregman divergence. Finally, we discuss the more general family of  $\phi$ -deformed logarithmic paths in App. G and show limiting behavior of various rho-tau Bregman divergences in App. H.

## A Annealed Importance Sampling

We briefly present annealed importance sampling (AIS) [60] as a representative example of an MCMC method where the choice of annealing path can play a crucial role [42, 54]. AIS relies on similar insights as the Jarzynski equality in nonequilibrium thermodynamics [44, 45], and may be used to estimate (log) normalization or partition functions or sample from complex distributions.

More concretely, consider an initial distribution  $\pi_0(x) \propto \tilde{\pi}_0(x)$  which is tractable to sample and is often chosen to have normalization constant  $\mathcal{Z}_0 = 1$ . We are often interested in estimating the normalizing constant  $\mathcal{Z}_1 = \int \tilde{\pi}_1(x)$  of a target distribution  $\pi_1(x) \propto \tilde{\pi}_1(x)$ , where only the unnormalized density  $\tilde{\pi}_1$  is available. Since direct sampling from  $\pi_0(x)$  may require prohibitive sample complexity to accurately estimate the normalization constant ratio  $\mathcal{Z}_1/\mathcal{Z}_0$  [20, 17], AIS decomposes the estimation problem into a sequence of easier subproblems using a *path* of intermediate distributions  $\{\tilde{\pi}_{\beta_t}(x)\}_{\beta_0=0}^{\beta_T=1}$  between the endpoints  $\tilde{\pi}_0(x)$  and  $\tilde{\pi}_1(x)$ . Most commonly, the geometric averaging path is used

$$\tilde{\pi}_{\beta_t}(x) = \frac{\tilde{\pi}_0(x)^{1-\beta_t} \tilde{\pi}_1(x)^{\beta_t}}{\mathcal{Z}(\beta_t)} \quad \text{where} \quad \mathcal{Z}(\beta_t) = \int \tilde{\pi}_0(x)^{1-\beta_t} \tilde{\pi}_1(x)^{\beta_t} dx. \quad (45)$$

AIS proceeds by constructing a sequence of Markov transition kernels  $\mathcal{T}_t(x_{t+1}|x_t)$  which leave  $\pi_{\beta_t}$  invariant, with  $\int \pi_{\beta_t}(x_t) \mathcal{T}_t(x_{t+1}|x_t) dx_t = \pi_{\beta_t}(x_{t+1})$ . Commonly, this is achieved using kernels such as HMC or Langevin dynamics [61] which transform the samples, with Metropolis-Hastings accept-reject steps to ensure invariance. To interpret AIS as importance sampling in an extended state space [60, 17], we define the reverse kernel as  $\tilde{\mathcal{T}}_t(x_t|x_{t+1}) = \frac{\pi_{\beta_t}(x_t) \mathcal{T}_t(x_{t+1}|x_t)}{\int \pi_{\beta_t}(x_t) \mathcal{T}_t(x_{t+1}|x_t) dx}$ . Using the invariance of  $\mathcal{T}_t$ , we observe that  $\pi_{\beta_t}(x_{t+1}) \tilde{\mathcal{T}}_t(x_t|x_{t+1}) = \pi_{\beta_t}(x_t) \mathcal{T}_t(x_{t+1}|x_t)$ .

To construct an estimator of  $\mathcal{Z}_T/\mathcal{Z}_0$  using AIS, we sample from  $x_0 \sim \pi_0(x)$ , run the transition kernels in the forward direction to obtain samples  $x_{1:T}$ , and

calculate the importance sampling weights along the path,

$$w(x_{0:T}) = \frac{\tilde{\pi}_1(x_T) \prod_{t=0}^{T-1} \tilde{\mathcal{T}}_t(x_t | x_{t+1})}{\tilde{\pi}_0(x_0) \prod_{t=0}^{T-1} \mathcal{T}_t(x_{t+1} | x_t)} = \prod_{t=1}^T \frac{\tilde{\pi}_{\beta_t}(x_t)}{\tilde{\pi}_{\beta_{t-1}}(x_t)} = \prod_{t=1}^T \left( \frac{\pi_T(x_t)}{\pi_0(x_t)} \right)^{\beta_t - \beta_{t-1}}. \quad (46)$$

Note that we have used the above identity relating  $\mathcal{T}_t$  and  $\tilde{\mathcal{T}}_t$  in the second equality, and the definition of the geometric averaging path in the last equality.

Finally, it can be shown that  $w(x_{0:T})$  provides an unbiased estimator of  $\mathcal{Z}_1/\mathcal{Z}_0$ , with  $\mathbb{E}[w(x_{0:T})] = \mathcal{Z}_1/\mathcal{Z}_0$  [60]. We can thus estimate the partition function ratio using the empirical average over  $K$  annealing chains,  $\mathcal{Z}_1/\mathcal{Z}_0 \approx \frac{1}{K} \sum w_{0:T}^{(k)}$ . We detail the complete AIS procedure in [Alg. 1](#).

AIS is considered among the gold standard methods for estimating normalization constants. Closely related MCMC methods involving path sampling [38] include Sequential Monte Carlo [28], which may involve resampling steps to prioritize higher-probability  $x_t$ , or parallel tempering [30], which runs  $T$  parallel sampling chains in order to obtain accurate samples from each  $\pi_{\beta_t}(x)$ .

## B Proof of [Thm. 1](#)

In the main text and below, we present and prove [Thm. 1](#) in terms of scalar inputs and decomposable Bregman divergences. As we show in [App. B.2](#) [Thm. 3](#), a similar Bregman divergence-minimization interpretation of quasi-arithmetic means holds for vector-valued inputs, where the representation function is applied element-wise. Most commonly, vectorized divergences are constructed between parameter vectors  $\boldsymbol{\theta}$  of some (deformed) exponential family. However, we argue in [App. C](#) that these cases are best understood using representations of unnormalized densities as in [Thm. 1](#) and the  $\rho$ -affine property of parametric families. Nevertheless, we provide proof of [Thm. 3](#) for completeness.

**Theorem 1 (Rho-Tau Bregman Information)** *Consider a monotonic representation function  $\rho : \mathcal{X}_\rho \subset \mathbb{R} \mapsto \mathcal{Y}_\rho \subset \mathbb{R}$  and a convex function  $f : \mathcal{Y}_\rho \rightarrow \mathbb{R}$ . Consider discrete mixture weights  $\boldsymbol{\beta} = \{\beta_i\}_{i=1}^N$  over  $N$  inputs  $\boldsymbol{\pi}(x) = \{\pi_i(x)\}_{i=1}^N$ ,  $\pi_i(x) \in \mathcal{X}_\rho$ , with  $\sum_i \beta_i = 1$ . Finally, assume the expected value  $\mu_\rho(\boldsymbol{\pi}, \boldsymbol{\beta}) := \sum_{i=1}^N \beta_i \rho(\tilde{\pi}_i(x)) \in \text{ri}(\mathcal{Y}_\rho)$  is in the relative interior of the range of  $\rho$  for all  $x \in \mathcal{X}$ . Then, we have the following results,*

(i) *For a given Bregman divergence  $D_f[\rho(\tilde{\pi}_a) : \rho(\tilde{\pi}_b)]$  with generator  $\Psi_f$ , the optimization*

$$\mathcal{I}_{f,\rho}(\tilde{\boldsymbol{\pi}}, \boldsymbol{\beta}) := \min_{\mu} \sum_{i=1}^N \beta_i D_f[\rho(\tilde{\pi}_i) : \rho(\mu)]. \quad (15)$$

*has a unique minimizer given by the quasi-arithmetic mean with representation function  $\rho(\tilde{\pi})$*

$$\mu_\rho^*(\tilde{\boldsymbol{\pi}}, \boldsymbol{\beta}) = \rho^{-1} \left( \sum_{i=1}^N \beta_i \rho(\tilde{\pi}_i) \right) = \arg \min_{\mu} \sum_{i=1}^N \beta_i D_f[\rho(\tilde{\pi}_i) : \rho(\mu)].$$

The arithmetic mean is recovered for  $\rho(\tilde{\pi}_i) = \tilde{\pi}_i$  and any  $f$  [11].

(ii) At this minimizing argument, the value of the expected divergence in Eq. (15) is called the Rho-Tau Bregman Information and is equal to a gap in Jensen's inequality for the convex functional  $\Psi[\rho_{\tilde{\pi}}] = \int f(\rho_{\tilde{\pi}}(x))dx$ , mixture weights  $\beta$ , and inputs  $\tilde{\pi}$ ,

$$\mathcal{I}_{f,\rho}(\tilde{\pi}, \beta) = \sum_{i=1}^N \beta_i \Psi_f[\rho(\tilde{\pi}_i)] - \Psi_f[\rho(\mu_{\rho}^*)]. \quad (16)$$

(iii) Using  $\mu \neq \mu_{\rho}^*(\tilde{\pi}, \beta)$  as the representative in Eq. (15), the suboptimality gap is a rho-tau Bregman divergence

$$D_{f,f^*}[\rho(\mu_{\rho}^*) : \tau(\mu)] = \sum_{i=1}^N \beta_i D_f[\rho(\tilde{\pi}_i) : \rho(\mu)] - \mathcal{I}_{f,\rho}(\tilde{\pi}, \beta) \quad (17)$$

where  $D_{f,f^*}[\rho(\mu^*) : \tau(\mu)] = D_f[\rho(\mu^*) : \rho(\mu)] = D_{f^*}[\tau(\mu) : \tau(\mu^*)]$ .

*Proof (ii):* We first show the optimal representative  $\mu^* = \rho^{-1}(\sum_{i=1}^N \beta_i \rho(\tilde{\pi}_i))$  yields a Jensen diversity in (ii), before proving this choice is the unique minimizing argument.

Expanding the expected divergence in Eq. (15) for  $\mu = \mu^*$ , we have  $\sum_{i=1}^N \beta_i D_F[\rho(\tilde{\pi}_i) : \rho(\mu^*)] = \sum_{i=1}^N \beta_i \Psi_f[\rho(\tilde{\pi}_i)] - \Psi_f[\rho(\mu^*)] - \int (\sum_{i=1}^N \beta_i \rho(\tilde{\pi}_i) - \rho(\mu^*)) \tau(\mu^*) dx$ . Since  $\sum_i \beta_i \rho(\tilde{\pi}_i) = \rho(\mu^*)$ , the final term cancels to yield

$$\sum_{i=1}^N \beta_i D_F[\rho(\tilde{\pi}_i) : \rho(\mu^*)] = \sum_{i=1}^N \beta_i \Psi_f[\rho(\tilde{\pi}_i)] - \Psi_f[\rho(\mu^*)]. \quad (47)$$

**(i):** For any other representative  $\mu$ , we write the difference in expected divergence and use Eq. (47) to simplify,

$$\sum_{i=1}^N \beta_i D_F[\rho(\tilde{\pi}_i) : \rho(\mu)] - \sum_{i=1}^N \beta_i D_F[\rho(\tilde{\pi}_i) : \rho(\mu^*)] \quad (48)$$

$$= \sum_{i=1}^N \underbrace{\beta_i \Psi_f[\rho(\tilde{\pi}_i)]}_{\Psi_f[\rho(\mu)]} - \Psi_f[\rho(\mu^*)] - \int \left( \sum_{i=1}^N \beta_i \rho(\tilde{\pi}_i(x)) - \rho(\mu(x)) \right) \tau(\mu(x)) dx \quad (49)$$

$$\begin{aligned} & - \left( \sum_{i=1}^N \underbrace{\beta_i \Psi_f[\rho(\tilde{\pi}_i)]}_{\Psi_f[\rho(\mu^*)]} - \Psi_f[\rho(\mu^*)] \right) \\ & = \Psi_f[\rho(\mu^*)] - \Psi_f[\rho(\mu)] - \int (\rho(\mu^*(x)) - \rho(\mu(x))) \tau(\mu(x)) dx \\ & = D_F[\rho(\mu^*) : \rho(\mu)]. \end{aligned} \quad (50)$$

where we note that  $\rho(\mu^*) = \sum_{i=1}^N \beta_i \rho(\tilde{\pi}_i)$ . The rho-tau divergence is minimized if and only if  $\rho(\mu^*) = \rho(\mu)$  [86], thus proving (i).

**(iii):** Finally, we can express the suboptimality gap in Eq. (48) or rho-tau Bregman divergence in Eq. (50) as the gap in a conjugate optimization.

Considering the conjugate expansion of  $\Psi_f[\rho(\mu^*)]$ , we have

$$\begin{aligned}\Psi_f[\rho(\mu^*)] &= \sup_{\tau(\mu)} \int \rho(\mu^*(x)) \tau(\mu(x)) dx - \Psi_{f^*}^*[\tau(\mu)] \\ &\geq \int \rho(\mu^*(x)) \tau(\mu(x)) dx - \Psi_{f^*}^*[\tau(\mu)]\end{aligned}\quad (51)$$

for any choice of  $\tau(\mu)$ . This provides a lower bound on  $\Psi[\rho(\mu^*)]$ , where the gap in the lower bound is the canonical form of the Bregman divergence. Indeed, substituting  $\Psi_{f^*}^*[\tau(\mu)] = \int \rho(\mu(x)) \tau(\mu(x)) dx - \Psi_f[\rho(\mu)]$  in Eq. (48), we have

$$\begin{aligned}D_F[\rho(\mu_\rho(\tilde{\pi}, \beta)) : \rho(\mu)] &= \Psi_f[\rho(\mu^*)] + \Psi_{f^*}^*[\tau(\mu)] - \int \rho(\mu^*(x)) \tau(\mu(x)) dx \\ &= \Psi_f[\rho(\mu^*)] - \Psi_f[\rho(\mu)] - \int (\rho(\mu^*(x)) - \rho(\mu(x))) \tau(\mu(x)) dx. \quad \square\end{aligned}$$

B.1 Interpretations of Thm. 1(iii):

Conjugate optimizations which treat  $f$ -divergences as a convex function of one argument are popular for providing variational lower bounds on divergences [62, 73] or min-max optimizations for adversarial training [69, 68]. Note however, that this proof provides a variational *upper* bound on the Bregman Information, which includes the Jensen-Shannon divergence (Example 3) and mutual information (Banerjee et al. [11] Ex. 6) as examples. To our knowledge, this upper bound has not been used extensively in the literature.

The equality in Eq. (17) can also be interpreted as a generalized bias-variance tradeoff for Bregman divergences ([18] Sec. 21, [71, 1]).

## B.2 Vector Bregman Divergence Minimization & Quasi-Arithmetic Means

A more standard setting is to consider a finite-dimensional Bregman divergence over a vector of inputs, such as the natural parameters  $\boldsymbol{\theta}$  of a (deformed) exponential family  $\tilde{\pi}_{\boldsymbol{\theta}}^{(q)}(x) = g(x) \exp_q\{\langle \boldsymbol{\theta}, \mathbf{T}(x) \rangle\}$ . However, we argue that this setting is best captured in our representational framework (see App. C), using  $\rho(\tilde{\pi}_{\boldsymbol{\theta}}^{(q)}(x)) = \log_q \frac{\tilde{\pi}_{\boldsymbol{\theta}}^{(q)}(x)}{g(x)} = \langle \boldsymbol{\theta}, \mathbf{T}(x) \rangle = \sum_{j=1}^d \theta^j T^j(x)$  and the  $\rho$ -linearity of the density with respect to the appropriate base measure.

Nevertheless, we would also like to extend Thm. 1 to hold for  $N$  vector-valued,  $d$ -dimensional inputs.

**Theorem 3** Consider a collection of inputs  $\mathbf{u} = \{\mathbf{u}_i\}_{i=1}^N$  where  $\mathbf{u}_i = \{u_i^1, \dots, u_i^j, \dots, u_i^d\}_{j=1}^d$ . In this case, consider applying the monotonic representation function  $\rho : \mathcal{X}_\rho^d \subset \mathbb{R}^d \rightarrow \mathcal{Y}_\rho^d \subset \mathbb{R}^d$  elementwise  $\rho(\mathbf{u}_i) := \{\rho(u_i^1), \dots, \rho(u_i^j), \dots, \rho(u_i^d)\}_{j=1}^d$ . For a convex generating function  $F : \mathcal{Y}_\rho^d \subset \mathbb{R}^d \rightarrow \mathbb{R}$ , define the Bregman divergence as

$$D_F[\rho(\mathbf{u}_a) : \rho(\mathbf{u}_b)] = F(\rho(\mathbf{u}_a)) - F(\rho(\mathbf{u}_b)) - \langle \rho(\mathbf{u}_a) - \rho(\mathbf{u}_b), \nabla_\rho F(\rho(\mathbf{u}_b)) \rangle$$

where the inner product sums over dimensions  $1 \leq j \leq d$ . Using analogous definition of a conjugate representation as in Section 2.2, we have  $\tau(\mathbf{u}) = \nabla_\rho F(\rho(\mathbf{u}))$  with  $\tau(u^j) = \frac{\partial}{\partial(\rho(\mathbf{u}))^j} F(\rho(\mathbf{u}))$ .

Finally, consider discrete mixture weights  $\boldsymbol{\beta} = \{\beta_i\}_{i=1}^N$  with  $\sum_i \beta_i = 1$ , and assume the expected value  $\mu_\rho(\mathbf{u}, \boldsymbol{\beta}) := \sum_{i=1}^N \beta_i \rho(\mathbf{u}_i) \in \text{ri}(\mathcal{Y}_\rho^d)$  is in the relative interior of the range of  $\rho$ . Then, we have the following results,

(i) For a Bregman divergence with generator  $F$ , the optimization

$$\mathcal{I}_{F,\rho}(\mathbf{u}, \boldsymbol{\beta}) := \min_{\boldsymbol{\mu}} \sum_{i=1}^N \beta_i D_F[\rho(\mathbf{u}_i) : \rho(\boldsymbol{\mu})]. \quad (52)$$

has a unique minimizer given by the quasi-arithmetic mean with representation function  $\rho(\tilde{\pi})$

$$\boldsymbol{\mu}_\rho^*(\mathbf{u}, \boldsymbol{\beta}) = \rho^{-1} \left( \sum_{i=1}^N \beta_i \rho(\mathbf{u}_i) \right) = \arg \min_{\boldsymbol{\mu}} \sum_{i=1}^N \beta_i D_F[\rho(\mathbf{u}_i) : \rho(\boldsymbol{\mu})].$$

The arithmetic mean is recovered for  $\rho(\mathbf{u}_i) = \mathbf{u}_i$  and any  $F$  [11].

(ii) At this minimizing argument, the value of the expected divergence in Eq. (52) is called the Rho-Tau Bregman Information and is equal to a gap in Jensen's inequality for the convex function  $F$ , mixture weights  $\boldsymbol{\beta}$ , and inputs  $\mathbf{u} = \{\mathbf{u}_i\}_{i=1}^N$ ,

$$\mathcal{I}_{F,\rho}(\mathbf{u}, \boldsymbol{\beta}) = \sum_{i=1}^N \beta_i F(\rho(\mathbf{u}_i)) - F(\rho(\boldsymbol{\mu}_\rho^*)). \quad (53)$$

(iii) Using  $\boldsymbol{\mu} \neq \boldsymbol{\mu}_\rho^*(\mathbf{u}, \boldsymbol{\beta})$  as the representative in Eq. (52), the suboptimality gap is a rho-tau Bregman divergence

$$D_F[\rho(\boldsymbol{\mu}_\rho^*) : \rho(\boldsymbol{\mu})] = \sum_{i=1}^N \beta_i D_F[\rho(\mathbf{u}_i) : \rho(\boldsymbol{\mu})] - \mathcal{I}_{F,\rho}(\mathbf{u}, \boldsymbol{\beta}). \quad (54)$$

*Proof (ii):* Again, we start by showing that the optimal representative  $\boldsymbol{\mu}_\rho^* = \rho^{-1}(\sum_{i=1}^N \beta_i \rho(\mathbf{u}_i))$  yields a Jensen diversity in (ii). Expanding the expected divergence in Eq. (52) for  $\boldsymbol{\mu} = \boldsymbol{\mu}_\rho^*$ , we have  $\sum_{i=1}^N \beta_i D_F[\rho(\mathbf{u}_i) : \rho(\boldsymbol{\mu}_\rho^*)] = \sum_{i=1}^N \beta_i F(\rho(\mathbf{u}_i)) - F(\rho(\boldsymbol{\mu}_\rho^*)) - \langle \sum_{i=1}^N \beta_i \rho(\mathbf{u}_i) - \rho(\boldsymbol{\mu}_\rho^*), \tau(\boldsymbol{\mu}_\rho^*) \rangle$ . Since  $\sum_i \beta_i \rho(\mathbf{u}_i) = \rho(\boldsymbol{\mu}_\rho^*)$ , the final term cancels to yield

$$\sum_{i=1}^N \beta_i D_F[\rho(\mathbf{u}_i) : \rho(\boldsymbol{\mu}_\rho^*)] = \sum_{i=1}^N \beta_i F(\rho(\mathbf{u}_i)) - F(\rho(\boldsymbol{\mu}_\rho^*)). \quad (55)$$

**(i, iii):** Writing the difference in expected divergence for a suboptimal representative  $\mu$  and using Eq. (55), we have

$$\begin{aligned} & \sum_{i=1}^N \beta_i D_F [\rho(\mathbf{u}_i) : \rho(\mu)] - \sum_{i=1}^N \beta_i D_F [\rho(\mathbf{u}_i) : \rho(\mu_\rho^*)] \\ &= \sum_{i=1}^N \beta_i F(\rho(\mathbf{u}_i)) - F(\rho(\mu)) - \left\langle \sum_{i=1}^N \beta_i \rho(\mathbf{u}_i) - \rho(\mu), \tau(\mu) \right\rangle - \left( \sum_{i=1}^N F(\rho(\mathbf{u}_i)) - F(\rho(\mu_\rho^*)) \right) \\ &= D_F [\rho(\mu_\rho^*) : \rho(\mu)]. \end{aligned} \quad (56)$$

The rho-tau divergence is minimized iff  $\rho(\mu_\rho^*) = \rho(\mu)$  [86], thus proving (i).

### C Parametric Bregman Divergence and Annealing Paths within (Deformed) Exponential Families

Consider a  $q$ -exponential family with a  $d$ -dimensional natural parameter vector  $\theta \in \Theta \subset \mathbb{R}^d$ , sufficient statistic vector  $\mathbf{T}(x)$ , and base density  $g(x)$ ,

$$\begin{aligned} \pi_{\theta}^{(q)}(x) &= \frac{1}{\mathcal{Z}_q(\theta)} g(x) \exp_q \{ \langle \theta, \mathbf{T}(x) \rangle \} \\ \text{where } \mathcal{Z}_q(\theta) &= \int g(x) \exp_q \{ \langle \theta, \mathbf{T}(x) \rangle \} dx. \end{aligned} \quad (57)$$

We let  $\tilde{\pi}_{\theta}^{(q)}(x) = g(x) \exp_q \{ \langle \theta, \mathbf{T}(x) \rangle \}$  denote the unnormalized density, often abbreviating to  $\tilde{\pi}_{\theta}(x)$  for convenience.

From the convexity of  $\exp_q$ , it can be shown that the normalization constant  $\mathcal{Z}_q(\theta)$  is a convex function of the parameters  $\theta$ , with first derivative

$$\frac{\partial \mathcal{Z}_q(\theta)}{\partial \theta^j} = \int g(x) [1 + (1-q)\theta \cdot \mathbf{T}(x)]^{\frac{q}{1-q}} \cdot T^j(x) dx = \int g(x)^{1-q} \tilde{\pi}_{\theta}(x) (x)^q \cdot T^j(x) dx \quad (58)$$

We show that the Bregman divergence induced by  $\frac{1}{q} \mathcal{Z}_q(\theta)$ , for  $q > 0$ , corresponds to the Amari  $\alpha$ -divergence between parametric unnormalized densities,

$$\begin{aligned} D_{\frac{1}{q} \mathcal{Z}_q} [\theta' : \theta] &= \frac{1}{q} \mathcal{Z}_q(\theta') - \frac{1}{q} \mathcal{Z}_q(\theta) - \langle \nabla \frac{1}{q} \mathcal{Z}_q(\theta), \theta' - \theta \rangle \\ &= \frac{1}{q} \mathcal{Z}_q(\theta') - \frac{1}{q} \mathcal{Z}_q(\theta) - \frac{1}{q} \int g(x)^{1-q} \tilde{\pi}_{\theta}(x)^q \left( \langle \theta', \mathbf{T}(x) \rangle - \langle \theta, \mathbf{T}(x) \rangle \right) dx \\ &\stackrel{(1)}{=} \frac{1}{q} \mathcal{Z}_q(\theta') - \frac{1}{q} \mathcal{Z}_q(\theta) - \frac{1}{q} \int g(x)^{1-q} \tilde{\pi}_{\theta}(x)^q \left( \log_q \frac{\tilde{\pi}_{\theta'}(x)}{g(x)} - \log_q \frac{\tilde{\pi}_{\theta}(x)}{g(x)} \right) dx \\ &= \frac{1}{q} \mathcal{Z}_q(\theta') - \frac{1}{q} \mathcal{Z}_q(\theta) - \frac{1}{q(1-q)} \int g(x)^{1-q} \tilde{\pi}_{\theta}(x)^q \left( \frac{\tilde{\pi}_{\theta'}(x)^{1-q}}{g(x)} - \frac{\tilde{\pi}_{\theta}(x)^{1-q}}{g(x)} \right) dx \\ &= \frac{1}{q} \mathcal{Z}_q(\theta') - \frac{1}{q} \mathcal{Z}_q(\theta) - \frac{1}{q(1-q)} \int \left( \tilde{\pi}_{\theta'}(x)^{1-q} \tilde{\pi}_{\theta}(x)^q dx + \frac{1}{q(1-q)} \int \tilde{\pi}_{\theta}(x) dx \right) \\ &= \frac{1}{q} \int \tilde{\pi}_{\theta'}(x) dx + \frac{1}{1-q} \int \tilde{\pi}_{\theta}(x) dx - \frac{1}{q(1-q)} \int \tilde{\pi}_{\theta'}(x)^{1-q} \tilde{\pi}_{\theta}(x)^q dx \\ &= D_A^{(q)} [\tilde{\pi}_{\theta'} : \tilde{\pi}_{\theta}] \end{aligned} \quad (59)$$

where in (1) we use the fact that  $\log_q \frac{\tilde{\pi}_{\theta}(x)}{g(x)} = \langle \theta, \mathbf{T}(x) \rangle$ .

**Bregman Divergence within Deformed Exponential Family** Consider a deformed  $q$ -exponential family [80, 58] with natural parameters  $\boldsymbol{\theta} = \{\theta^i\}_{j=1}^d$ , sufficient statistics  $\mathbf{T}(x) = \{T^j(x)\}_{j=1}^d$ , and partition function  $\mathcal{Z}_q(\boldsymbol{\theta})$ .

$$\pi_{\boldsymbol{\theta}}^{(q)}(x) = \frac{1}{\mathcal{Z}_q(\boldsymbol{\theta})} g(x) \exp_q\{\langle \boldsymbol{\theta}, \mathbf{T}(x) \rangle\} \quad \text{where } \mathcal{Z}_q(\boldsymbol{\theta}) = \int \tilde{\pi}_{\boldsymbol{\theta}}^{(q)}(x) dx. \quad (60)$$

The standard Bregman divergence, with  $\boldsymbol{\theta} \in \Theta \subset \mathbb{R}^d$  as input, is

$$D_{\mathcal{Z}}[\boldsymbol{\theta}' : \boldsymbol{\theta}] = D_{\text{KL}}[\tilde{\pi}_{\boldsymbol{\theta}} : \tilde{\pi}_{\boldsymbol{\theta}'}] \quad D_{\frac{1}{q}\mathcal{Z}_q}[\boldsymbol{\theta}' : \boldsymbol{\theta}] = D_A^{(q)}[\tilde{\pi}_{\boldsymbol{\theta}'} : \tilde{\pi}_{\boldsymbol{\theta}}] \quad (61)$$

where we define the Amari  $\alpha$ -divergence in Eq. (3).

Similarly to Example 1, we may also view this as a decomposable divergence in the  $\log_q$ -representation  $\rho(\tilde{\pi}_{\boldsymbol{\theta}}^{(q)}) = \log_q \frac{\tilde{\pi}_{\boldsymbol{\theta}}^{(q)}(x)}{g(x)} = \langle \boldsymbol{\theta}, \mathbf{T}(x) \rangle$ , with

$$\rho(\tilde{\pi}_{\boldsymbol{\theta}}^{(q)}) = \log_q \frac{\tilde{\pi}_{\boldsymbol{\theta}}^{(q)}(x)}{g(x)} \quad f(\rho) = \frac{1}{q} (\exp_q\{\rho\} - \rho - 1) \quad (62)$$

$$\Psi_f[\rho_{\tilde{\pi}}] = -\frac{1}{q} \int \langle \boldsymbol{\theta}, \mathbf{T}(x) \rangle dx + \frac{1}{q} \mathcal{Z}_q(\boldsymbol{\theta}) - \frac{1}{q}. \quad (63)$$

Note that the order of the  $\alpha$ -divergence is set by the deformation parameter  $q$  in the definition of the representation function  $\rho_q$  or  $q$ -exponential family.

We have used this Bregman divergence minimization to interpret the  $q$ -paths between *arbitrary* endpoint densities from a parametric perspective in Section 4.2 Example 11.

**Bregman Divergence within Exponential Family** For  $q = 1$  and the exponential family,

$$\mathcal{Z}(\boldsymbol{\theta}) = \int \tilde{\pi}_{\boldsymbol{\theta}}(x) dx = \int g(x) \exp\{\langle \boldsymbol{\theta}, \mathbf{T}(x) \rangle\} dx \quad (64)$$

$$\nabla \mathcal{Z}(\boldsymbol{\theta}) = \left\{ \int \tilde{\pi}_{\boldsymbol{\theta}}(x) T^j(x) dx \right\}_{j=1}^d = \left\{ \int g(x) \exp\{\langle \boldsymbol{\theta}, \mathbf{T}(x) \rangle\} T^j(x) dx \right\}_{j=1}^d,$$

which leads to the Bregman divergence

$$\begin{aligned} D_{\mathcal{Z}}[\boldsymbol{\theta}' : \boldsymbol{\theta}] &= \mathcal{Z}(\boldsymbol{\theta}') - \mathcal{Z}(\boldsymbol{\theta}) - \langle \nabla \mathcal{Z}(\boldsymbol{\theta}), \boldsymbol{\theta}' - \boldsymbol{\theta} \rangle \\ &= \mathcal{Z}(\boldsymbol{\theta}') - \mathcal{Z}(\boldsymbol{\theta}) - \int \tilde{\pi}_{\boldsymbol{\theta}}(x) \langle \boldsymbol{\theta}', \mathbf{T}(x) \rangle dx - \int \tilde{\pi}_{\boldsymbol{\theta}}(x) \langle \boldsymbol{\theta}, \mathbf{T}(x) \rangle dx \\ &= \int \tilde{\pi}_{\boldsymbol{\theta}'}(x) dx - \int \tilde{\pi}_{\boldsymbol{\theta}}(x) dx - \int \tilde{\pi}_{\boldsymbol{\theta}}(x) \left( \log \tilde{\pi}_{\boldsymbol{\theta}'}(x) - \log \tilde{\pi}_{\boldsymbol{\theta}}(x) \right) dx \\ &= D_{\text{KL}}[\tilde{\pi}_{\boldsymbol{\theta}}(x) : \tilde{\pi}_{\boldsymbol{\theta}'}(x)]. \end{aligned} \quad (65)$$

By contrast, the divergence generated by the *log* partition function  $\log \mathcal{Z}(\boldsymbol{\theta})$  yields the KL divergence between normalized distributions. Since

$$\frac{\partial}{\partial \theta^j} \log \mathcal{Z}(\boldsymbol{\theta}) = \frac{1}{\mathcal{Z}(\boldsymbol{\theta})} \int \tilde{\pi}_{\boldsymbol{\theta}}(x) T^j(x) dx = \int \pi_{\boldsymbol{\theta}}(x) T^j(x) dx,$$

we have

$$\begin{aligned}
D_{\log \mathcal{Z}}[\boldsymbol{\theta}' : \boldsymbol{\theta}] &= \log \mathcal{Z}(\boldsymbol{\theta}') - \log \mathcal{Z}(\boldsymbol{\theta}) - \langle \nabla \log \mathcal{Z}(\boldsymbol{\theta}), \boldsymbol{\theta}' - \boldsymbol{\theta} \rangle \\
&= \log \mathcal{Z}(\boldsymbol{\theta}') - \log \mathcal{Z}(\boldsymbol{\theta}) - \int \pi_{\boldsymbol{\theta}}(x) \langle \boldsymbol{\theta}' - \boldsymbol{\theta}, \mathbf{T}(x) \rangle dx \\
&= \log \int \tilde{\pi}_{\boldsymbol{\theta}'}(x) dx - \log \int \tilde{\pi}_{\boldsymbol{\theta}}(x) dx - \int \pi_{\boldsymbol{\theta}}(x) \left( \log \tilde{\pi}_{\boldsymbol{\theta}'}(x) - \log \tilde{\pi}_{\boldsymbol{\theta}}(x) \right) dx \\
&= D_{\text{KL}}[\pi_{\boldsymbol{\theta}}(x) : \pi_{\boldsymbol{\theta}'}(x)].
\end{aligned} \tag{66}$$

### C.1 Annealing Paths between (Deformed) Exponential Family Endpoints

The above Bregman divergences can be used to analyze annealing paths in the special case where the endpoint densities  $\tilde{\pi}_{\boldsymbol{\theta}_0}$  and  $\tilde{\pi}_{\boldsymbol{\theta}_1}$  belong to the same (deformed) exponential family, with base density  $g(x)$ , natural parameters  $\boldsymbol{\theta} = \{\theta^j\}_{j=1}^d$ , sufficient statistics  $\mathbf{T}(x) = \{T^j(x)\}_{j=1}^d$ , and log partition function  $\psi(\boldsymbol{\theta})$ ,

$$\pi_{\boldsymbol{\theta}}^{(q)}(x) = \frac{1}{\mathcal{Z}_q(\boldsymbol{\theta})} g(x) \exp_q\{\langle \boldsymbol{\theta}, \mathbf{T}(x) \rangle\} \quad \text{where } \mathcal{Z}_q(\boldsymbol{\theta}) = \int \tilde{\pi}_{\boldsymbol{\theta}}^{(q)}(x) dx. \tag{67}$$

#### Example 15 (Annealing within (Deformed) Exponential Families)

Due to the  $\rho$ -affine property of deformed exponential families, it is natural to consider the  $\rho(\tilde{\pi}) = \log_q \tilde{\pi}$  path within the  $\exp_q$  family.

Ignoring the normalization constant, the unnormalized density with respect to  $g(x)$  is linear in  $\boldsymbol{\theta}$  after applying the  $\rho(\tilde{\pi}_{\boldsymbol{\theta}}) = \log \frac{\tilde{\pi}_{\boldsymbol{\theta}}(x)}{g(x)}$  representation function, with  $\log \frac{\tilde{\pi}_{\boldsymbol{\theta}}(x)}{g(x)} = \langle \boldsymbol{\theta}, \mathbf{T}(x) \rangle$ . Since the quasi-arithmetic mean also has this  $\rho$ -affine property (Eq. (5)), we can see that the  $q$ -path or geometric path between (deformed) exponential endpoints  $\tilde{\pi}_{\boldsymbol{\theta}_0}(x)$  and  $\tilde{\pi}_{\boldsymbol{\theta}_1}(x)$  is simply a linear interpolation in the natural parameters

$$\boldsymbol{\theta}_\beta = (1 - \beta) \boldsymbol{\theta}_0 + \beta \boldsymbol{\theta}_1 = \arg \min_{\boldsymbol{\theta}_r} (1 - \beta) D_{\frac{1}{q} \mathcal{Z}_q}[\boldsymbol{\theta}_0 : \boldsymbol{\theta}_r] + \beta D_{\frac{1}{q} \mathcal{Z}_q}[\boldsymbol{\theta}_1 : \boldsymbol{\theta}_r].$$

which includes the KL divergence and exponential family for  $q = 1$ .

**Example 16 (Moment Averaging Path of Grosse et al. [42])** In the case of the standard exponential family,

$$\pi_{\boldsymbol{\theta}}(x) = g(x) \exp\{\langle \boldsymbol{\theta}, \mathbf{T}(x) \rangle - \psi(\boldsymbol{\theta})\} \text{ with } \psi(\boldsymbol{\theta}) = \log \int g(x) \exp\{\langle \boldsymbol{\theta}, \mathbf{T}(x) \rangle\} dx,$$

Grosse et al. [42] propose the *moment averaging* path, which uses the dual parameter mapping  $\rho(\boldsymbol{\theta}) = \boldsymbol{\eta}(\boldsymbol{\theta}) = \mathbb{E}_{\pi_{\boldsymbol{\theta}}}[\mathbf{T}(x)]$  as a representation function for the quasi-arithmetic mean,

$$\boldsymbol{\eta}(\boldsymbol{\theta}_\beta) = (1 - \beta) \boldsymbol{\eta}(\boldsymbol{\theta}_0) + \beta \boldsymbol{\eta}(\boldsymbol{\theta}_1) = \arg \min_{\boldsymbol{\eta}_r} (1 - \beta) D_{\psi^*}[\boldsymbol{\eta}_0 : \boldsymbol{\eta}_r] + \beta D_{\psi^*}[\boldsymbol{\eta}_1 : \boldsymbol{\eta}_r]$$

for an appropriate dual divergence based on the dual of the log partition function  $\psi^*(\boldsymbol{\eta}(\boldsymbol{\theta})) = D_{\text{KL}}[\pi_{\boldsymbol{\theta}}(x) : g(x)]$  (see [42]). While Grosse et al. [42] show performance gains using the moment averaging path, additional sampling procedures may be required to find  $\boldsymbol{\theta}_\beta$  via the inverse mapping  $\boldsymbol{\eta}^{-1}(\cdot)$ .

## D $f$ -Divergence as Rho-Tau Divergence

While we have only considered unnormalized densities with respect to the base measure  $dx$  so far, we might also consider densities with respect to an arbitrary base measure  $\nu_0$ . Letting  $\tilde{\pi} = \frac{d\mu}{d\nu_0}$  denote the Radon-Nikodym derivative of the measure  $\mu$  with respect to  $\nu_0$ , we can rewrite the Bregman divergence in the  $\tau(\tilde{\pi}) = \tilde{\pi}$  representation as

$$D_{f^*} \left[ \frac{d\mu_a}{d\nu_0} : \frac{d\mu_b}{d\nu_0} \right] = \int f^* \left( \frac{d\mu_a}{d\nu_0}(x) \right) - f^* \left( \frac{d\mu_b}{d\nu_0}(x) \right) - \left( \frac{d\mu_a}{d\nu_0}(x) - \frac{d\mu_b}{d\nu_0}(x) \right) f^{*\prime} \left( \frac{d\mu_b}{d\nu_0} \right) d\nu_0.$$

The family of  $f$ -divergences  $I_{f^*}[\mu_a : \mu_b]$  [26, 3] is a fundamental example of a decomposable divergence, which is invariant to the base measure  $\nu_0$  and monotonic under coarse-graining ([6] Ch. 3). Assuming the standard form of the convex generating function  $f^*(1) = f^{*\prime}(1) = 0$ , any  $f$ -divergence can be written as a decomposable Bregman divergence for densities with respect to the measure in the second argument

$$I_{f^*}[\mu_a : \mu_b] := \int f^* \left( \frac{d\mu_a}{d\mu_b}(x) \right) d\mu_b(x) \quad (68)$$

$$= D_{f^*} \left[ \frac{d\mu_a}{d\mu_b} : 1 \right] \quad (69)$$

$$= \int \left( f^* \left( \frac{d\mu_a}{d\mu_b}(x) \right) - f^*(1) - \left( \frac{d\mu_a}{d\mu_b}(x) - 1 \right) f^{*\prime}(1) \right) d\mu_b(x).$$

Our results for decomposable Bregman divergences may also be translated to results for  $f$ -divergences using the above reasoning.

A crucial example of the  $f$ -divergence is Zhang's  $(\alpha, \beta)$ -divergence, which we presented as a Bregman Information in [Example 7](#). This is the unique family of base measure-invariant divergences satisfying the homogeneity condition  $D[c\tilde{\pi}_a : c\tilde{\pi}_b] = cD[\tilde{\pi}_a : \tilde{\pi}_b]$  (see [43] pg. 68, [5]), and includes the KL divergence, Amari  $\alpha$ -divergence, and (weighted) Jensen-Shannon divergences as special cases. See Zhang [86] Sec. 3.5-6 for further discussion.

**$\alpha$ -Divergence in the  $\tau$ -Identity Representation** It is well-known that the  $\alpha$ -divergence is an  $f$ -divergence, although we derived it as a representational Bregman divergence for  $\rho(\tilde{\pi}) = \log_q \tilde{\pi}$  and  $\tau(\tilde{\pi}) = \log_{1-q} \tilde{\pi}$  in [Example 5](#). However, we reasoned above that the  $f$ -divergence should be derivable from the  $\tau(\tilde{\pi}) = \tilde{\pi}$  representation with the appropriate choice of base measure.

Recall that the  $\tau$ -identity representation was used to derive the Beta divergence in [Example 6](#). In particular, consider the  $\rho(\tilde{\pi}) = \log_q \tilde{\pi}$  and  $\tau(\tilde{\pi}) = \tilde{\pi}$  representations with  $f^*(\tau) = \frac{1}{1-q} \frac{1}{2-q} \tau^{2-q} - \frac{1}{1-q} \tau + \frac{1}{2-q}$ . Taking  $\mu_b$  to be the base measure with  $\tilde{\pi}_b = \frac{d\mu_b}{dx}$ , the Beta divergence becomes

$$\begin{aligned} D_{f^*} \left[ \frac{d\mu_a}{d\mu_b} : 1 \right] &= \frac{1}{1-q} \frac{1}{2-q} \int \left( \frac{d\mu_a}{d\mu_b} \right)^{2-q} d\mu_b - \frac{1}{1-q} \int \frac{d\mu_a}{d\mu_b} d\mu_b + \frac{1}{2-q} \int d\mu_b \\ &= \frac{1}{q-1} \int \tilde{\pi}_a(x) dx + \frac{1}{2-q} \int \tilde{\pi}_b(x) dx - \frac{1}{q-1} \frac{1}{2-q} \int \tilde{\pi}_a(x)^{2-q} \tilde{\pi}_b(x)^{q-1} dx \end{aligned}$$

which we recognize as an Amari  $\alpha$ -divergence for  $\alpha = q-1$

$$D_A^{(\alpha)}[\tilde{\pi}_a : \tilde{\pi}_b] = \frac{1}{\alpha} \int \tilde{\pi}_a(x) dx + \frac{1}{1-\alpha} \int \tilde{\pi}_b(x) dx - \frac{1}{\alpha} \frac{1}{1-\alpha} \int \tilde{\pi}_a(x)^{1-\alpha} \tilde{\pi}_b(x)^\alpha dx$$

For  $q = \alpha + 1$ , we recover the Amari divergence of order  $\alpha$ , which corresponds to the  $\rho(\tilde{\pi}) = \log_{\alpha+1} \tilde{\pi}$  representation.

## E Information Geometry from Divergence Functions

The ‘Eguchi relations’, from the seminal work of Eguchi [31, 32], show that a statistical divergence  $D[\pi_a : \pi_b]$  naturally induces a Riemannian metric and pair of conjugate affine connections on the tangent space of a manifold  $\mathcal{M}$  of probability densities. We first review the Eguchi relations for the parametric case, where the parameters  $\boldsymbol{\theta}(\pi) : \mathcal{M}_{\boldsymbol{\theta}} \mapsto \Theta \subset \mathbb{R}^N$  provide a coordinate system for points  $\pi_{\boldsymbol{\theta}} \in \mathcal{M}_{\boldsymbol{\theta}}$  on the manifold, before reviewing the nonparametric information geometry of Zhang [87], where each point  $\tilde{\pi} \in \mathcal{M}$  on the manifold is represented by its (infinite-dimensional) density function.

### E.1 Parametric Information Geometry

In coordinate notation with basis vectors of the tangent space  $\partial_i = \frac{\partial}{\partial \theta^i}$ , the metric  $g_{ij}(\boldsymbol{\theta}) = \langle \partial_i, \partial_j \rangle$  specifies a bilinear form at a point indexed by  $\boldsymbol{\theta}$ . An affine connection  $\nabla$  defines notions of curvature (of the manifold), covariant differentiation (of vector fields), and parallel transport (of tangent vectors along curves). In particular, the covariant derivative can be expressed using the (scalar) Christoffel symbols  $\Gamma_{ij,k}(\boldsymbol{\theta}) = \langle \nabla_{\partial_i} \partial_j, \partial_k \rangle$ . We refer to Amari and Nagaoka [7] or Nielsen [63] for detailed background.

For a given divergence function, taking the second and third order differentials yield the following metric and conjugate pair of affine connections

$$g_{ij}(\boldsymbol{\theta}) = -(\partial_j)_{\pi_{\boldsymbol{\theta}_a}} (\partial_k)_{\pi_{\boldsymbol{\theta}_b}} D[\pi_{\boldsymbol{\theta}_a} : \pi_{\boldsymbol{\theta}_b}] \Big|_{\pi_{\boldsymbol{\theta}_a} = \pi_{\boldsymbol{\theta}_b}} \quad (70)$$

$$\Gamma_{ij,k}(\boldsymbol{\theta}) = -(\partial_i)_{\pi_{\boldsymbol{\theta}_a}} (\partial_j)_{\pi_{\boldsymbol{\theta}_a}} (\partial_k)_{\pi_{\boldsymbol{\theta}_b}} D[\pi_{\boldsymbol{\theta}_a} : \pi_{\boldsymbol{\theta}_b}] \Big|_{\pi_{\boldsymbol{\theta}_a} = \pi_{\boldsymbol{\theta}_b}} \quad (71)$$

$$\Gamma_{ij,k}^*(\boldsymbol{\theta}) = -(\partial_i)_{\pi_{\boldsymbol{\theta}_b}} (\partial_j)_{\pi_{\boldsymbol{\theta}_b}} (\partial_k)_{\pi_{\boldsymbol{\theta}_a}} D[\pi_{\boldsymbol{\theta}_a} : \pi_{\boldsymbol{\theta}_b}] \Big|_{\pi_{\boldsymbol{\theta}_a} = \pi_{\boldsymbol{\theta}_b}} \quad (72)$$

where  $(\partial_j)_{\pi_{\boldsymbol{\theta}_a}}$  indicates partial differentiation with respect to the parameter  $\theta_a^j$  of the first argument. Note that conjugacy of connections amounts to  $\Gamma_{ij,k} + \Gamma_{ik,j}^* = \partial_i g_{jk}$  and ensures the inner product of tangent vectors is preserved by parallel translation of each vector according to the respective connection (Amari and Nagaoka [7] Sec. 3.1).

It can be shown that *any*  $f$ -divergence [31], including the KL divergence in either direction, Amari’s  $\alpha$ -divergence, and the Jensen-Shannon divergence<sup>3</sup>, yields the Fisher Information metric, which is the unique metric that is invariant to reparameterization [21],

$$\begin{aligned} g_{ij}(\boldsymbol{\theta}) &= \int \pi_{\boldsymbol{\theta}}(x) \frac{\partial \log \pi_{\boldsymbol{\theta}}(x)}{\partial \theta^i} \frac{\partial \log \pi_{\boldsymbol{\theta}}(x)}{\partial \theta^j} dx = \int \frac{\partial \log \pi_{\boldsymbol{\theta}}(x)}{\partial \theta^i} \frac{\partial \pi_{\boldsymbol{\theta}}(x)}{\partial \theta^j} dx \quad (73) \\ &= \int \frac{\partial \log_q \pi_{\boldsymbol{\theta}}(x)}{\partial \theta^i} \frac{\partial \log_{1-q} \pi_{\boldsymbol{\theta}}(x)}{\partial \theta^j} dx, \end{aligned}$$

<sup>3</sup> The JSD, rescaled by  $\frac{1}{\beta(1-\beta)}$  to ensure the standard form that  $f''(1) = 1$ , is also an  $f$ -divergence for  $f_{\beta}(u) = \frac{1}{\beta(1-\beta)} ((1-\beta)u \log u + ((1-\beta)u + \beta) \log ((1-\beta)u + \beta))$ .

where the expression in terms of  $q$ -representations reflects the duality of representation functions [7, 86, 63] in the  $\tau$ -deformed gauge (see Sec. 4.1). However, the divergences we consider will differ in their induced dual affine connections (Eguchi [31], Zhang [87]; Table 2).

**Bregman Divergence and KL Divergence** It is well-known that any Bregman divergence induces a *dually flat* space, in which there exists a coordinate system such that either  $\Gamma_{ij,k}$  or  $\Gamma_{ij,k}^*$  vanishes everywhere (Amari and Nagaoka [7] Ch. 3, Nielsen [63] Sec. 3.7, Amari [6] Ch. 6). It is easy to confirm that  $\Gamma_{ij,k}(\boldsymbol{\theta}) = 0$  for the parametric Bregman divergence  $D_\psi[\boldsymbol{\theta}_a : \boldsymbol{\theta}_b] = D_{\text{KL}}[\pi_{\boldsymbol{\theta}_b} : \pi_{\boldsymbol{\theta}_a}]$  (Eq. (64)) associated with the exponential family.

For arbitrary input distributions, differentiating the reverse KL divergence ( $\alpha \rightarrow 1$ ) using  $-(\partial_i)_a(\partial_j)_a(\partial_k)_b D_{\text{KL}}[\pi_b : \pi_a]$ , we obtain

$$\Gamma_{ij,k}(\boldsymbol{\theta}) = \Gamma_{ij,k}^{(1)}(\boldsymbol{\theta}) := \int \frac{\partial^2 \log \pi_{\boldsymbol{\theta}}(x)}{\partial \theta^i \partial \theta^j} \frac{\partial \pi_{\boldsymbol{\theta}}(x)}{\partial \theta^k} dx \quad (74)$$

$$\Gamma_{ij,k}^*(\boldsymbol{\theta}) = \Gamma_{ij,k}^{(0)}(\boldsymbol{\theta}) := \int \frac{\partial^2 \pi_{\boldsymbol{\theta}}(x)}{\partial \theta^i \partial \theta^j} \frac{\partial \log \pi_{\boldsymbol{\theta}}(x)}{\partial \theta^k} dx. \quad (75)$$

These dual connections are well-known as the  $e$ - and  $m$ -connections, respectively [7]. Similarly, the forward KL divergence ( $\alpha \rightarrow 0$ ) induces  $\Gamma_{ij,k} = \Gamma_{ij,k}^{(0)}$  and  $\Gamma_{ij,k}^* = \Gamma_{ij,k}^{(1)}$ .

**$\alpha$ -Connection and  $f$ -Divergence** More generally, Amari [4] introduced the family of  $\alpha$ -connections which, among other interpretations, may be viewed as an arithmetic mixture of  $\Gamma_{ij,k}^{(1)}$  and  $\Gamma_{ij,k}^{(0)}$ ,

$$\begin{aligned} \Gamma_{ij,k}^{(\alpha)}(\boldsymbol{\theta}) &= (1 - \alpha) \Gamma_{ij,k}^{(0)} + \alpha \Gamma_{ij,k}^{(1)} =: \langle \nabla_{\partial_i}^{(\alpha)} \partial_j, \partial_k \rangle \\ &= \int \frac{1}{\pi_{\boldsymbol{\theta}}(x)} \left( \frac{\partial^2 \pi_{\boldsymbol{\theta}}(x)}{\partial \theta^i \partial \theta^j} \frac{\partial \pi_{\boldsymbol{\theta}}(x)}{\partial \theta^k} - \alpha \frac{1}{\pi_{\boldsymbol{\theta}}(x)} \frac{\partial \pi_{\boldsymbol{\theta}}(x)}{\partial \theta^i} \frac{\partial \pi_{\boldsymbol{\theta}}(x)}{\partial \theta^j} \frac{\partial \pi_{\boldsymbol{\theta}}(x)}{\partial \theta^k} \right) dx \end{aligned} \quad (76)$$

where the second line can be derived by simplifying from Eq. (74)-(75). Adapted to our notation, it can be shown that any  $f$ -divergence induces a pair of conjugate connections  $\Gamma_{ij,k} = \Gamma_{ij,k}^{(\alpha)}$  and  $\Gamma_{ij,k}^* = \Gamma_{ij,k}^{(1-\alpha)}$  where  $\alpha = -f'''(1) - 1$  (see Table 2).

In particular, we see that both the  $\alpha$ -divergence and the (weighted, scaled) Jensen-Shannon divergence induce the  $\alpha$ -connection. Although the limiting behavior as  $\alpha \rightarrow \{0, 1\}$  recovers the KL divergence for both divergences, note that the  $f$ -divergence generator for the  $\alpha$ -divergence in Eq. (3) is a function of the representation  $\rho_q(u) = \log_q(u)$  with  $\alpha = q$ . By contrast, the JSD can be derived as either a Jensen diversity or  $f$ -divergence as a function of the the mixture parameter  $\beta$ .

## E.2 Information Geometry of Rho-Tau Divergences

**Parametric Case** Zhang [86, 87] use the Eguchi relations to analyze the geometry induced by the representational  $\alpha$ -divergence, or scaled Bregman Information, in Eq. (20). For a given choice of  $\rho$ ,  $\tau$ , and  $\beta$ , viewing  $\frac{1}{\beta(1-\beta)} \mathcal{I}_{f,\rho}(\tilde{\boldsymbol{\pi}}, \boldsymbol{\beta})$

Divergence	$\alpha(\beta, \rho, \tau)$ for $\Gamma(\tilde{\pi})$	$\alpha(\beta, \rho, \tau)$ for $\Gamma^*(\tilde{\pi})$	Outer Integration
$D_f[\rho(\tilde{\pi}_a) : \rho(\tilde{\pi}_b)]$	$-\frac{\rho''(\tilde{\pi})}{\rho'(\tilde{\pi})}$	$-\frac{\tau''(\tilde{\pi})}{\tau'(\tilde{\pi})}$	$\rho'(\tilde{\pi})\tau'(\tilde{\pi})$
$\frac{1}{\beta(1-\beta)}\mathcal{I}_{f,\rho}(\tilde{\pi}, \beta)$	$-(1-\beta)\frac{\tau''(\tilde{\pi})}{\tau'(\tilde{\pi})} + \beta\frac{\rho''(\tilde{\pi})}{\rho'(\tilde{\pi})}$	$-(1-\beta)\frac{\rho''(\tilde{\pi})}{\rho'(\tilde{\pi})} + \beta\frac{\tau''(\tilde{\pi})}{\tau'(\tilde{\pi})}$	$\rho'(\tilde{\pi})\tau'(\tilde{\pi})$
(all $\alpha(\beta, \rho, \tau)$ below omit a $\tilde{\pi}^{-1}$ factor)			
$D_{\text{KL}}[\tilde{\pi}_b : \tilde{\pi}_a] (q=1)$	1	0	$\tilde{\pi}^{-1}$
$D_A^{(\alpha)}[\tilde{\pi}_a : \tilde{\pi}_b] (\frac{q=1}{\beta=\alpha})$	$\beta$	$1-\beta$	$\tilde{\pi}^{-1}$
$D_A^{(\alpha)}[\tilde{\pi}_a : \tilde{\pi}_b] (\frac{q=\alpha}{\beta=1})$	$q$	$1-q$	$\tilde{\pi}^{-1}$
$D_Z^{(\beta,q)}[\tilde{\pi}_b : \tilde{\pi}_a]$	$(1-\beta)(1-q) + \beta q$	$(1-\beta)q + \beta(1-q)$	$\tilde{\pi}^{-1}$
$D_{\text{KL}}[\tilde{\pi}_a : \tilde{\pi}_b] (q=0)$	0	1	$\tilde{\pi}^{-1}$
$\frac{1}{\alpha(1-\alpha)}D_{\text{JS}}^{(\alpha)}[\tilde{\pi}_b : \tilde{\pi}_a] (\frac{q=0}{\beta=\alpha})$	$1-\beta$	$\beta$	$\tilde{\pi}^{-1}$
$D_B^{(1-q)}[\tilde{\pi}_b : \tilde{\pi}_a]$	$q$	0	$\tilde{\pi}^{-q}$
$\frac{1}{\beta(1-\beta)} \text{Breg. Info } D_B^{(1-q)}$	$\beta q$	$(1-\beta)q$	$\tilde{\pi}^{-q}$
$D_C^{(q,\lambda)}[\tilde{\pi}_a : \tilde{\pi}_b]$	$q$	$1-\lambda$	$\tilde{\pi}^{\lambda-1-q}$
$\frac{1}{\beta(1-\beta)} \text{Breg. Info } D_C^{(q,\lambda)}$	$(1-\beta)(1-\lambda) + \beta q$	$(1-\beta)q + \beta(1-\lambda)$	$\tilde{\pi}^{\lambda-1-q}$

Table 2: Dual pair of affine connections induced by divergence functions considered in Sec. 4, where  $\alpha(\beta, \rho, \tau)$  refers to Eq. (78) for primal and dual connections  $\Gamma(\tilde{\pi})$  and  $\Gamma^*(\tilde{\pi})$ . The factor  $\rho'(\tilde{\pi})\tau'(\tilde{\pi})$  also specifies the Riemannian metric in Eq. (77). See App. E for detailed background. In each pair of rows, we list the rho-tau Bregman divergence  $D_f[\rho(\tilde{\pi}_a) : \rho(\tilde{\pi}_b)]$  and induced Bregman Information, where values of  $q$  indicate the order of  $\rho(\tilde{\pi}) = \log_q(\tilde{\pi})$ . We ensure  $f$ -divergences  $I_f$ , including  $\frac{1}{\beta(1-\beta)}D_{\text{JS}}^{(\beta)}$ , are in standard form with  $f''(1) = 1$ .

as a divergence functional  $D_{f,\rho}^{(\beta)}[\pi_0 : \pi_1]$  yields the Riemannian metric and primal affine connection (expressed using the Christoffel symbols  $\Gamma_{ij,k}(\boldsymbol{\theta})$ ) as,

$$g_{ij}(\boldsymbol{\theta}) = \int \frac{\partial \rho_{\pi_{\boldsymbol{\theta}}}(x)}{\partial \theta^i} \frac{\partial \tau_{\pi_{\boldsymbol{\theta}}}(x)}{\partial \theta^j} dx = \int \rho'_{\pi_{\boldsymbol{\theta}}}(x) \tau'_{\pi_{\boldsymbol{\theta}}}(x) \frac{\partial \pi_{\boldsymbol{\theta}}(x)}{\partial \theta^i} \frac{\partial \pi_{\boldsymbol{\theta}}(x)}{\partial \theta^j} dx, \quad (77)$$

$$\begin{aligned} \Gamma_{ij,k}(\boldsymbol{\theta}) &= \int \rho'_{\pi_{\boldsymbol{\theta}}} \tau'_{\pi_{\boldsymbol{\theta}}} \left( \frac{\partial^2 \pi_{\boldsymbol{\theta}}}{\partial \theta^i \partial \theta^j} \frac{\partial \pi_{\boldsymbol{\theta}}}{\partial \theta^k} - \alpha(x; \rho, \tau, \beta) \frac{\partial \pi_{\boldsymbol{\theta}}}{\partial \theta^i} \frac{\partial \pi_{\boldsymbol{\theta}}}{\partial \theta^j} \frac{\partial \pi_{\boldsymbol{\theta}}}{\partial \theta^k} \right) dx \\ &\text{where } \alpha(x; \rho, \tau, \beta) = -(1-\beta) \frac{\tau''_{\pi_{\boldsymbol{\theta}}}(x)}{\tau'_{\pi_{\boldsymbol{\theta}}}(x)} - \beta \frac{\rho''_{\pi_{\boldsymbol{\theta}}}(x)}{\rho'_{\pi_{\boldsymbol{\theta}}}(x)}. \end{aligned} \quad (78)$$

which generalizes the Fisher Information metric and standard  $\alpha$ -connections for  $\rho(\pi) = \log(\pi)$ ,  $\tau(\pi) = \pi$ , and  $\alpha(x; \rho, \tau, \beta) = \alpha \cdot \pi_{\boldsymbol{\theta}}(x)^{-1}$ . For  $\beta \neq \{0, 1\}$  and given  $\rho$  and  $\tau$ , note that the primal connection  $\Gamma_{ij,k}(\boldsymbol{\theta})$  is a mixture  $\Gamma_{ij,k}^{(\beta)}(\boldsymbol{\theta}) = (1-\beta)\Gamma_{ij,k}^{(0)}(\boldsymbol{\theta}) + \beta\Gamma_{ij,k}^{(1)}(\boldsymbol{\theta})$  of the conjugate connections induced by the rho-tau Bregman divergences ( $\beta = 0$  or  $1$ ). Zhang [87] derive similar expressions for nonparametric statistical manifolds where each point is represented by arbitrary density function  $\tilde{\pi}$ , with tangent vectors  $u(x), v(x)$  replacing the basis vectors for the tangent space  $\frac{\partial \pi_{\boldsymbol{\theta}}}{\partial \theta^i}, \frac{\partial \pi_{\boldsymbol{\theta}}}{\partial \theta^j}$  in the parametric case (see App. E.2).

In Table 2, we summarize the metric and dual affine connections derived from the various examples of the (scaled) rho-tau Bregman Information that we consider in Sec. 4.

**Nonparametric Statistical Manifolds** Since the target density in MCMC applications is usually unnormalized and can not be represented using a parametric model, we would like to consider a nonparametric information geometry over the space of positive, unnormalized measures. In this case, the approach is to construct a Banach manifold  $\mathcal{M}_{\nu_0}$  of all densities which are absolutely continuous with respect to a base measure  $\nu_0$  [72, 51]. Similarly to our likelihood ratio interpretation in Eq. (34), the coordinate mappings correspond to  $q$ -logarithmic likelihood ratios, while the tangent space can be identified with all one-dimensional  $q$ -exponential families with base measure  $\tilde{\pi}_0$  [51]. For detailed constructions over *normalized* nonparametric distributions, see Loaiza and Quiceno [51, 52] or Pistone and Sempi [72], Gibilisco and Pistone [39], Grasselli [41]. Extension to a nonparametric manifold of *unnormalized* densities should be straightforward, but remains for future work.

Assuming the manifold and tangent spaces are well-defined, Zhang [86, 87] obtain the following analogues of the Fisher metric and  $\alpha$ -connection. For general tangent vectors  $u(x), v(x), w(x)$  at a point  $\tilde{\pi}(x)$ ,

$$g_{u,v}(\tilde{\pi}) = \langle u, v \rangle = \int \rho'_{\tilde{\pi}}(x) \tau'_{\tilde{\pi}}(x) u(x) v(x) dx \quad (79)$$

$$\begin{aligned} \Gamma_{w u, v}^{(\beta)}(\tilde{\pi}) &= \langle \nabla_w^{(\beta)} u, v \rangle \\ &= \int \rho'_{\tilde{\pi}}(x) \tau'_{\tilde{\pi}}(x) \left( (d_w u(x)) v(x) + \left( (1 - \beta) \frac{\tau''_{\tilde{\pi}}(x)}{\tau'_{\tilde{\pi}}(x)} + \beta \frac{\rho''_{\tilde{\pi}}(x)}{\rho'_{\tilde{\pi}}(x)} \right) u(x) w(x) v(x) \right) dx. \end{aligned} \quad (80)$$

where  $d_w u$  is the directional derivative of  $u$  in the direction of  $w$  and  $\rho'_{\tilde{\pi}}(x) = \rho'(\tilde{\pi}(x))$ . The parametric expression above can be recovered using, for example,  $u(x) = \frac{\partial}{\partial \theta^i} \pi_{\theta}(x)$ , and we also note the similar form of Eq. (80) to the expression in Eq. (76). Again, the connections  $\Gamma_{w u, v}^{(\beta)} = (1 - \beta) \Gamma_{w u, v}^{(0)} + \beta \Gamma_{w u, v}^{(1)}$  are obtained as mixtures of the conjugate connections induced by the rho-tau Bregman divergence.

## F Geodesics for the Rho-Tau Bregman Divergence

In this section, we show that the quasi-arithmetic mixture path in the  $\rho(\tilde{\pi})$  representation of densities is a geodesic with respect to the primal connection induced by the rho-tau divergence  $D_f[\rho(\tilde{\pi}_1) : \rho(\tilde{\pi}_0)]$ . Recall from Zhang [87] Sec. 2.3 (Eq. 88) that the  $\alpha$ -connection (or covariant derivative) associated with the rho-tau Bregman divergence has the form

$$\begin{aligned} \nabla_{\dot{\gamma}}^{(\alpha)} \dot{\gamma} &= (d_{\dot{\gamma}} \dot{\gamma})_{\gamma_t} + \frac{d}{d\gamma} (\alpha \log \rho'(\gamma_t) + (1 - \alpha) \log \tau'(\gamma_t)) \cdot \dot{\gamma}^2 \\ &= (d_{\dot{\gamma}} \dot{\gamma})_{\gamma_t} + \left( \alpha \frac{\rho''(\gamma_t)}{\rho'(\gamma_t)} + (1 - \alpha) \frac{\tau''(\gamma_t)}{\tau'(\gamma_t)} \right) \cdot \dot{\gamma}^2 \end{aligned} \quad (81)$$

where  $\dot{\gamma} = \frac{d\gamma}{dt}$  and the parameter  $\alpha$  plays the role of the convex combination or mixture parameter  $\beta$ . In this section, we use the notation  $\nabla^{(\alpha)}$  to represent the

affine connection, instead of the Christoffel symbol notation from e.g. Eq. (80), with  $\Gamma_{wu,v}^{(\alpha)}(\tilde{\pi}) = \langle \nabla_w^{(\alpha)} u, v \rangle$ .

We are interested in the Bregman divergence and  $\nabla^{(1)}$  connection for  $\alpha = 1$ . Using Eq. (5), we need to show that the geodesic equation  $\nabla_{\dot{\gamma}}^{(1)} \dot{\gamma} = 0$  holds (Nielsen [63] Sec. 3.12) for curves which are linear in the  $\rho$ -representation.

**Theorem 2** (Geodesics for Rho-Tau Bregman Divergence) *The curve  $\gamma_t = \rho^{-1}((1-t)\rho(\tilde{\pi}_0) + t\rho(\tilde{\pi}_1))$  (with time derivative  $\dot{\gamma}_t = \frac{d}{dt}\gamma_t$ ) is auto-parallel with respect to the primal affine connection  $\nabla^{(1)}$  induced by the rho-tau Bregman divergence  $D_f[\rho(\tilde{\pi}_a) : \rho(\tilde{\pi}_b)]$  for  $\beta = 1$ . In other words, the following geodesic equation holds*

$$\nabla_{\dot{\gamma}_t}^{(1)} \dot{\gamma}_t = d_{\dot{\gamma}_t} \dot{\gamma}_t + (\dot{\gamma}_t)^2 \cdot \left( \frac{\rho''(\gamma_t)}{\rho'(\gamma_t)} \right) = 0. \quad (21)$$

The  $\rho$ -representation of the unnormalized density thus provides an affine coordinate system for the geometry induced by  $D_f[\rho(\tilde{\pi}_a) : \rho(\tilde{\pi}_b)]$ .

*Proof* We simplify each of the terms in the geodesic equation, where we rewrite the desired geodesic equation in Eq. (21) to match Eq. 88 of Zhang [87],

$$\nabla_{\dot{\gamma}}^{(1)} \dot{\gamma} = d_{\dot{\gamma}} \dot{\gamma} + (\dot{\gamma})^2 \cdot \left( \frac{d}{d\gamma} \log \rho'(\gamma) \right) = 0 \quad (82)$$

First, note the particularly simple expression for  $\frac{d\rho(\gamma_t)}{dt} = \rho(\tilde{\pi}_1) - \rho(\tilde{\pi}_0)$  given the definition  $\rho(\gamma(t)) = (1-t)\rho(\tilde{\pi}_0) + t\rho(\tilde{\pi}_1)$ . Noting the chain rule  $\frac{d\rho_t}{dt} = \frac{d\rho(\gamma_t)}{d\gamma} \frac{d\gamma_t}{dt}$ , we can rearrange to obtain an expression for  $\dot{\gamma}(t)$

$$\dot{\gamma}(t) = \frac{d\gamma(t)}{dt} = \left( \frac{d\rho(\gamma_t)}{d\gamma} \right)^{-1} \frac{d\rho(\gamma_t)}{dt} = \left( \frac{d\rho(\gamma_t)}{d\gamma} \right)^{-1} (\rho(\tilde{\pi}_1) - \rho(\tilde{\pi}_0)) \quad (83)$$

Taking the directional derivative  $d_{\dot{\gamma}} \dot{\gamma} = \frac{d\dot{\gamma}}{d\gamma} \cdot \dot{\gamma}$ ,

$$\begin{aligned} d_{\dot{\gamma}_t} \dot{\gamma}_t &= \dot{\gamma}_t \cdot \frac{d}{d\gamma} \left[ \left( \frac{d\rho(\gamma_t)}{d\gamma} \right)^{-1} (\rho(\tilde{\pi}_1) - \rho(\tilde{\pi}_0)) \right] \\ &= -\dot{\gamma}_t (\rho(\tilde{\pi}_1) - \rho(\tilde{\pi}_0)) \frac{d\rho(\gamma_t)}{d\gamma}^{-2} \frac{d^2 \rho(\gamma_t)}{d\gamma^2} \end{aligned} \quad (84)$$

Rewriting the final term in Eq. (21), we have

$$\frac{d}{d\gamma} (\log \rho'(\gamma_t)) = \frac{d}{d\gamma} (\log \frac{d\rho(\gamma_t)}{d\gamma}) = \left( \frac{d\rho(\gamma_t)}{d\gamma} \right)^{-1} \frac{d^2 \rho(\gamma_t)}{d\gamma^2}. \quad (85)$$

Putting it all together, we have

$$\begin{aligned} \nabla_{\dot{\gamma}_t}^{(1)} \dot{\gamma}_t &= -\frac{d\dot{\gamma}_t}{d\gamma} \cdot \dot{\gamma}_t + (\dot{\gamma}_t)^2 \cdot \frac{d}{d\gamma} (\log \rho'(\gamma_t)) \\ &= -\dot{\gamma}_t (\rho(\tilde{\pi}_1) - \rho(\tilde{\pi}_0)) \frac{d\rho(\gamma_t)}{d\gamma}^{-2} \frac{d^2 \rho(\gamma_t)}{d\gamma^2} + (\dot{\gamma}_t)^2 \left( \frac{d\rho(\gamma_t)}{d\gamma} \right)^{-1} \frac{d^2 \rho(\gamma_t)}{d\gamma^2} \end{aligned} \quad (86)$$

Noting that  $\frac{d\rho(\gamma_t)}{d\gamma}^{-1} = \dot{\gamma}(\rho(\tilde{\pi}_1) - \rho(\tilde{\pi}_0))$  from Eq. (83), we have

$$\begin{aligned}\nabla_{\dot{\gamma}_t}^{(1)} \dot{\gamma}_t &= -\dot{\gamma}_t \frac{\rho(\tilde{\pi}_1) - \rho(\tilde{\pi}_0)}{\rho(\tilde{\pi}_1) - \rho(\tilde{\pi}_0)} \cdot \dot{\gamma}_t \frac{d\rho(\gamma_t)}{d\gamma}^{-1} \frac{d^2\rho(\gamma_t)}{d\gamma^2} + (\dot{\gamma}_t)^2 \left( \frac{d\rho(\gamma_t)}{d\gamma} \right)^{-1} \frac{d^2\rho(\gamma_t)}{d\gamma^2} \\ &= -(\dot{\gamma}_t)^2 \left( \frac{d\rho(\gamma_t)}{d\gamma} \right)^{-1} \frac{d^2\rho(\gamma_t)}{d\gamma^2} + (\dot{\gamma}_t)^2 \left( \frac{d\rho(\gamma_t)}{d\gamma} \right)^{-1} \frac{d^2\rho(\gamma_t)}{d\gamma^2} \\ &= 0\end{aligned}$$

which proves the proposition.  $\square$

### G $\phi$ -Deformed Logarithm Paths

For a strictly positive  $\phi(v)$ , [56, 57, 58] defines the  $\phi$ -deformed logarithm

$$\log_{\phi}(u) = \int_1^u \frac{1}{\phi(v)} dv \quad (87)$$

The natural logarithm  $\log u$  is recovered for  $\phi(v) = v$ , and the  $q$ -deformed logarithm is recovered for  $\phi(v) = v^q$ . Note that  $\log_{\phi}(\tilde{\pi}(x))$  is monotonically increasing and concave in  $\tilde{\pi}(x)$ , since  $\frac{d^2}{du^2} \log_{\phi}(u) = -\frac{1}{\phi(u)^2} < 0$ .

In order to define the inverse function  $\exp_{\phi}$  such that  $u = \exp_{\phi}(\log_{\phi}(u))$ , it appears we need to know the indefinite integral of  $1/\phi(v)$  in Eq. (87). Instead, the  $\phi$ -exponential can be defined using the integral of an additional function  $\psi(v) = \frac{d}{dv} \exp_{\phi}(v)$ , where

$$\exp_{\phi}(u) = 1 + \int_0^u \psi(v) dv \quad (88)$$

We then have the relationships [59]

$$\psi(u) = \phi(\exp_{\phi}(u)) \quad \phi(u) = \psi(\log_{\phi}(u)). \quad (89)$$

The  $\phi$ -deformed logarithmic path can now be written as

$$\tilde{\pi}_{\beta}(x) = \exp_{\phi}((1 - \beta) \log_{\phi}(\tilde{\pi}_0(x)) + \beta \log_{\phi}(\tilde{\pi}_1(x))) \quad (90)$$

Its gradient with respect to  $x$  is often necessary for taking MCMC transition steps, for example.

$$\frac{d}{dx} \tilde{\pi}_{\beta}(x) = \phi(\tilde{\pi}_{\beta}) \left( (1 - \beta) \frac{\tilde{\pi}_0(x)}{\phi(\tilde{\pi}_0(x))} \frac{d \log \tilde{\pi}_0(x)}{dx} + \beta \frac{\tilde{\pi}_1(x)}{\phi(\tilde{\pi}_1(x))} \frac{d \log \tilde{\pi}_1(x)}{dx} \right) \quad (91)$$

where, for the first term in the chain rule, we use  $\phi(\tilde{\pi}_{\beta}) = \psi(\log_{\phi}(\tilde{\pi}_{\beta}))$ . It remains an interesting direction for future work to further explore special cases of the deformed logarithm [47], or even to learn the deformation function  $\phi(u)$  with respect to a quantitative measure of sample quality [77]. For the latter approach, parameterizing  $\phi(u)$  using a strictly positive neural network would still require integration to obtain  $\log_{\phi}$ . If we were to instead directly parameterize  $\log_{\phi}(u)$  using an input-convex neural network [9], evaluating (one of) the function(s)  $\exp_{\phi}$ ,  $\log_{\phi}$ , or  $\psi$  to evaluate  $\tilde{\pi}_{\beta}(x)$  may still be challenging.

## H Limiting Behavior of Rho-Tau Divergences

In this section, we show that the limiting behavior of the functions generating the  $\alpha$ -divergence as a rho-tau Bregman divergence recovers the familiar generators for the KL divergence. Similar techniques can be used to derive the limiting behavior for the  $\beta$ -divergence choice of  $\rho, \tau, f$ , and  $f^*$  in [Table 3](#).

**$f, \rho$  Limiting Behavior as  $\mathbf{q} \rightarrow \mathbf{0}$ :** Recall the choices of  $\rho$  and  $f$  which generate the  $\alpha$ -divergence,

$$\begin{aligned}\rho_{\tilde{\pi}} &= \log_q \tilde{\pi}(x) = \frac{1}{1-q} \tilde{\pi}(x)^{1-q} - \frac{1}{1-q} \\ f(\rho) &= \frac{1}{q} \exp_q \{\rho\} - \frac{1}{q} \rho - \frac{1}{q} = \frac{1}{q} [1 + (1-q)\rho]_+^{\frac{1}{1-q}} - \frac{1}{q} \rho - \frac{1}{q}.\end{aligned}\quad (92)$$

Considering the limiting behavior of  $f(\rho)$  as  $q \rightarrow 0$ , note that both the denominator  $d(q) = q$  and numerator  $n(q) = [1 + (1-q) \cdot \rho]_+^{\frac{1}{1-q}} - \rho - 1$  have  $\lim_{q \rightarrow 0} d(q) = 0$ ,  $\lim_{q \rightarrow 0} n(q) = 0$  and are well defined away from  $q = 0$ . We can thus use L'Hôpital's rule to find

$$\lim_{q \rightarrow 0} f(\rho) = \lim_{q \rightarrow 0} \frac{n'(q)}{d'(q)} = \frac{1}{1} \cdot n'(q) \Big|_{q=0} \quad (93)$$

Differentiating  $n(q) = [1 + (1-q) \cdot \rho]_+^{\frac{1}{1-q}} - \rho - 1$  with respect to  $q$  using the identity  $\frac{d}{dq}(h(q)^{g(q)}) = \frac{d}{dq} e^{g(q) \log h(q)} = h(q)^{g(q)} \left( h'(q) \frac{g(q)}{h(q)} + g'(q) \log h(q) \right)$ ,

$$\begin{aligned}n'(q) \Big|_{q=0} &= [1 + (1-q)\rho]_+^{\frac{1}{1-q}} \left( -\rho \frac{\frac{1}{1-q}}{1 + (1-q)\rho} + \frac{1}{(1-q)^2} \log(1 + (1-q)\rho) \right) \Big|_{q=0} \\ &= (1+\rho) \left( -\frac{\rho}{1+\rho} + \log(1+\rho) \right)\end{aligned}$$

$$\implies \lim_{q \rightarrow 0} f(\rho) = (1+\rho) \log(1+\rho) - \rho \quad (94)$$

where  $\rho_{\tilde{\pi}}(x) = \log_0 \tilde{\pi}(x) = \tilde{\pi} - 1$  and  $1 + \rho = \tilde{\pi}(x)$ . The function  $f(\rho_{\tilde{\pi}}) = \tilde{\pi}(x) \log \tilde{\pi}(x) - \tilde{\pi}(x) + 1$  thus matches the Bregman generator for the negative Shannon entropy and KL divergence  $D_{\text{KL}}[\tilde{\pi}_a : \tilde{\pi}_b]$ . Indeed, the rho-tau Bregman divergence simplifies as

$$\begin{aligned}D_f[\rho_{\tilde{\pi}_a} : \rho_{\tilde{\pi}_b}] &= \int f(\rho_{\tilde{\pi}_a}(x)) - f(\rho_{\tilde{\pi}_b}(x)) - (\rho_{\tilde{\pi}_a}(x) - \rho_{\tilde{\pi}_b}(x)) \tau_{\tilde{\pi}_b}(x) dx \\ &= \int \tilde{\pi}_a(x) \log \tilde{\pi}_a(x) - \tilde{\pi}_a(x) - \tilde{\pi}_b(x) \log \tilde{\pi}_b(x) + \tilde{\pi}_b(x) - (\tilde{\pi}_a(x) - \tilde{\pi}_b(x)) \log \tilde{\pi}_b(x) dx \\ &= \int \tilde{\pi}_a(x) \log \frac{\tilde{\pi}_a(x)}{\tilde{\pi}_b(x)} dx - \int \tilde{\pi}_a(x) dx + \int \tilde{\pi}_b(x) dx = D_{\text{KL}}[\tilde{\pi}_a : \tilde{\pi}_b].\end{aligned}\quad (95)$$

**$f, \rho$  Limiting Behavior as  $\mathbf{q} \rightarrow \mathbf{1}$ :** For  $q \rightarrow 1$ , we directly reason that  $\rho_{\tilde{\pi}}(x) = \log \tilde{\pi}(x)$  and  $f(\rho) = \exp\{\rho\} - \rho - 1$ . This leads to the generator  $f(\rho_{\tilde{\pi}}(x)) = -\log \tilde{\pi}(x) + \tilde{\pi}(x) - 1$ , which matches the  $f$ -divergence generator of the KL divergence.

**$f^*, \tau$  Limiting Behavior as  $\mathbf{q} \rightarrow \mathbf{1}$ :** Recall the choices of  $\tau$  and  $f^*$  which generate the  $\alpha$ -divergence,

$$\tau_{\tilde{\pi}}(x) = \log_{1-q} \tilde{\pi}(x) = \frac{1}{q} \tilde{\pi}(x)^q - \frac{1}{q} \quad (96)$$

$\tau$ -Deformed	Convex $f, f^*$	$q \rightarrow 0$	$q \rightarrow 1$	$q = 2$
$\rho(\tilde{\pi}) = \log_q \tilde{\pi}$	$f(\rho) = c \exp_q \rho$	$D_{\text{KL}}[\tilde{\pi}_a : \tilde{\pi}_b]$	$D_{\text{KL}}[\tilde{\pi}_b : \tilde{\pi}_a]$	$D_{\chi^2}[\tilde{\pi}_b : \tilde{\pi}_a]$
$\tau(\tilde{\pi}) = \log_{1-q} \tilde{\pi}$	$f^*(\tau) = c \exp_{1-q} \rho$	$D_{\text{KL}}[\tilde{\pi}_b : \tilde{\pi}_a]$	$D_{\text{KL}}[\tilde{\pi}_a : \tilde{\pi}_b]$	$D_{\chi^2}[\tilde{\pi}_a : \tilde{\pi}_b]$
$\tau$ -id	Convex $f, f^*$	$q = 0$	$q \rightarrow 1$	$q \rightarrow 2$
$\rho(\tilde{\pi}) = \log_q \tilde{\pi}$	$f(\rho) = c(\exp_q \rho)^{2-q}$	$\frac{1}{2} \ \tilde{\pi}_a - \tilde{\pi}_b\ _2^2$	$D_{\text{KL}}[\tilde{\pi}_b : \tilde{\pi}_a]$	$D_{\text{IS}}[\tilde{\pi}_b : \tilde{\pi}_a]$
$\tau(\tilde{\pi}) = \tilde{\pi}$	$f^*(\tau) = c \log_{q-1} \tau$	$\frac{1}{2} \ \tilde{\pi}_a - \tilde{\pi}_b\ _2^2$	$D_{\text{KL}}[\tilde{\pi}_a : \tilde{\pi}_b]$	$D_{\text{IS}}[\tilde{\pi}_b : \tilde{\pi}_a]$

Table 3: Limiting Behavior in  $q$  for Amari  $\alpha$  ( $\tau$ -deformed) and Beta-divergences ( $\tau$ -id) as rho-tau Bregman Divergences. The  $\rho, f$  rows indicate the behavior of  $D_f[\rho(\tilde{\pi}_a) : \rho(\tilde{\pi}_b)]$ , and the  $\tau, f^*$  rows indicate the behavior of  $D_{f^*}[\tau(\tilde{\pi}_a) : \tau(\tilde{\pi}_b)]$ , with  $D_f[\rho(\tilde{\pi}_a) : \rho(\tilde{\pi}_b)] = D_{f^*}[\tau(\tilde{\pi}_b) : \tau(\tilde{\pi}_a)]$ . Note that  $D_{\chi^2}$  indicates Pearson's  $\chi^2$  divergence and  $D_{\text{IS}}$  indicates the Itakura-Saito divergence.

$$f^*(\tau) = \frac{1}{1-q} \exp_{1-q} \{\tau\} - \frac{1}{1-q} \tau - \frac{1}{1-q} = \frac{1}{1-q} [1 + q\tau]_+^{\frac{1}{q}} - \frac{1}{1-q} \tau - \frac{1}{1-q}$$

For  $q \rightarrow 1$ , we have  $\tau_{\tilde{\pi}}(x) = \tilde{\pi}(x) - 1$ .

To calculate  $\lim_{q \rightarrow 1} f^*(\tau)$ , we apply L'Hôpital's rule using similar reasoning as above for  $d(q) = \frac{1}{1-q}$  and  $n(q) = [1 + q\tau]^{\frac{1}{q}} - \tau - 1$ . We differentiate using  $\frac{d}{dq}(f(q)^{g(q)}) = \frac{d}{dq} e^{g(q) \log f(q)} = f(q)^{g(q)} (f'(q) \frac{g(q)}{f(q)} + g'(q) \log f(q))$  with  $g(q) = \frac{1}{q}$ ,  $f(q) = 1 + q\tau$  to obtain

$$\begin{aligned} \lim_{q \rightarrow 1} f^*(\tau) &= \lim_{q \rightarrow 1} \frac{n'(q)}{d'(q)} = \frac{1}{-1} \cdot n'(q) \Big|_{q=1} = -[1 + q\tau]^{\frac{1}{q}} \left( \tau \frac{\frac{1}{q}}{1 + q\tau} - \frac{1}{q^2} \log(1 + q\tau) \right) \Big|_{q=1} \\ &= -(1 + \tau) \left( \frac{\tau}{1 + \tau} - \log(1 + \tau) \right) \\ \implies \lim_{q \rightarrow 1} f^*(\tau) &= (1 + \tau) \log(1 + \tau) - \tau \end{aligned} \quad (97)$$

Using  $\tau_{\tilde{\pi}}(x) = \tilde{\pi}(x) - 1$  for  $q = 1$ , we have  $f^*(\tau_{\tilde{\pi}}(x)) = \tilde{\pi}(x) \log \tilde{\pi}(x) - \tilde{\pi}(x) + 1$ , which matches the pointwise negative Shannon entropy or the  $f$ -divergence generator for  $D_f[\tilde{\pi}_a : \tilde{\pi}_b] = D_{\text{KL}}[\tilde{\pi}_a : \tilde{\pi}_b]$ . Identical derivations as in Eq. (95) confirm that the rho-tau divergence recovers  $D_{f^*}[\tilde{\pi}_a : \tau_{\tilde{\pi}_b}] = D_{\text{KL}}[\tilde{\pi}_a : \tilde{\pi}_b]$ .

This observation is indicative of the *representational* duality with respect to the functions  $\rho(u) = \log_q u$  and  $\tau(t) = \log_{1-q} t$ . Clearly, switching  $q \rightarrow 1-q$  and  $1-q \rightarrow q$  switches the role of  $f, \rho$  and  $f^*, \tau$ , so that we obtain the same divergence using  $D_{f,\rho}^{(q)}[\tilde{\pi}_a : \tilde{\pi}_b]$  and  $D_{f^*,\tau}^{(1-q)}[\tilde{\pi}_a : \tilde{\pi}_b]$ . For example, we have seen that using  $q = 0$  for  $\rho(u)$  and  $q = 1$  for  $\tau(t)$  recover the same divergence.

**$f^*, \tau$  Limiting Behavior as  $q \rightarrow 0$ :** As above, for  $q \rightarrow 0$  we have  $\tau_{\tilde{\pi}}(x) = \log \tilde{\pi}(x)$  and  $f^*(\tau) = \exp\{\tau\} - \tau - 1$ . This leads to  $f^*(\tau_{\tilde{\pi}}(x)) = -\log \tilde{\pi}(x) + \tilde{\pi}(x) - 1$ , which matches the  $f$ -divergence generator of the KL divergence, with  $D_{\text{KL}}[\tilde{\pi}_b : \tilde{\pi}_a] = D_f[\tilde{\pi}_a : \tilde{\pi}_b] = D_{f,\rho}^{(q=1)}[\tilde{\pi}_a : \tilde{\pi}_b] = D_{f^*,\tau}^{(q=0)}[\tilde{\pi}_a : \tilde{\pi}_b]$ .